3D hotspots of marine litter in the Mediterranean: a modeling study

Javier Soto-Navarro[1], Gabriel Jordá[2], Salud Deudero[2], Carme Alomar[2], Ángel Amores[1] and Montserrat Compa[2].

[1]Mediterranean Institute for Advanced Studies (IMEDEA, UIB-CSIC). Mallorca, Spain.

[2]Spanish Oceanographic Institute – Balearic Oceanographic Centre (IEO-COB). Mallorca, Spain.

Abstract

The 3D dispersion of marine litter (ML) over the Mediterranean basin has been simulated using the velocity fields from a high resolution circulation model as base to run a 3D lagrangian model. Three simulations have been performed to mimic the evolution of ML with density lower, similar, or higher than seawater. In all cases a realistic distribution of ML sources was used. Our results show that the accumulation/dispersion areas of the floating and buoyancy neutral particles are practically the same, although the latter are distributed in the water column, 90% of them found in the photic layer. Regarding to the densest particles, they rapidly sink and reach the seafloor close to their source. The regions of higher temporal variability mostly coincide with the ML accumulation regions. Weak seasonal variability occurs at a sub-basin scale as a result of the particles redistribution induced by the seasonal variability of the current field.

Keywords: Marine pollution, Marine litter, Mediterranean Sea, Plastic pollution, Lagrangian models, 3D circulation.

1. Introduction

The pollution of the oceans due to plastic waste generates great concern for both the scientific community and society as a whole. In recent years, both political (national and international) and scientific initiatives have been developed to mitigate the consequences of the massive use

of plastics and its presence in the marine environment (see Maximenko et al. (2019) for a complete summary). The United Nations Environmental Program (UNEP) defines marine litter (ML) as any persistent, manufactured or processed solid material that is discarded, disposed of or abandoned in the marine or coastal environment (UNEP, 2009). These materials accumulate in both shallow and deep waters, and especially in closed basins such as the Mediterranean Sea (Barnes et al., 2009; Cózar et al., 2015). The most recent estimates show that between 4.8 and 12.7 million tons of plastic waste were dumped into the ocean in 2010, an amount that is expected to increase by one order of magnitude by 2025 if no measures are implemented to improve the waste management systems. In the case of the Mediterranean, it is estimated that around one hundred thousand tons of plastic waste enter each year (J. R. Jambeck et al., 2015). Despite legislative advances in prevention, illegal dumping as well as waste transportation to the open ocean from coastal areas and river mouths is a problem that is still far from being solved (UNEP / MAR, 2015)

This is an ecological concern as plastic waste is easily mistaken for food by marine animals causing important health problems, including death. Several studies have confirmed the harmful effects of ingestion of plastics in fish (Carson, 2013), turtles (Lazar and Gračan, 2011), cetaceans (Baulch and Perry, 2014) and seabirds (Azzarello and Van Vleet, 1987; Ryan and Jackson, 1987). In the Mediterranean Sea, coastal and offshore biodiversity has been reported to ingest plastics from micro to macro size (Deudero and Alomar, 2015; Compa et al., 2019). In addition to the direct effects on individuals, floating macro debris (> 25 mm) can become “vehicles” or “rafts” that are used by invasive species to travel long distances, accelerating their dispersion speed hence increasing their rate of invasion of new habitats and altering the recipient ecosystems (Aliani and Molcard, 2003; Barnes D. K., 2002). Furthermore, micro-plastics (< 5 mm) can contain contaminants added during their manufacturing processes or incorporated to their surfaces once in the marine environment (Koelmans et al., 2016). These contaminants associated to plastic ingestion by marine animals can be incorporated into food

webs and could eventually be transferred to humans causing toxicity, carcinogenesis, endocrine disruption and physical harm (Laist, 1997; Wright et al. 2013; Koch and Calafat, 2009; Mato et al., 2001). To these biological and ecological effects, we must add the socioeconomic impacts that the accumulation of waste on beaches and coastal areas has in the regions where the local economy strongly depends on coastal tourism (Compa et al., 2019b).

In the global ocean, studies based on both observations and numerical models have identified large areas of accumulation of floating debris located in each of the subtropical gyres on both sides of the equator (Eriksen et al., 2014; Law et al., 2014; Lebreton et al., 2012; Maximenko et al., 2012; Van Sebille et al., 2015). In the case of the Mediterranean, the observed concentrations are one of the highest in the world, comparable to the values found in subtropical gyres (Cózar et al., 2015). Unfortunately, at present a full description of ML distribution in marine environments solely based on observations is unfeasible. Due to the technical difficulties involved, measurement campaigns are usually restricted to regions near the coast, and are not carried out systematically, but during specific periods in which weather conditions are favorable for navigation (Arcangeli et al., 2018; Cózar et al., 2015; Faure et al., 2015; Gajšt et al., 2016; Ruiz-Orejón et al., 2016; Schmidt et al., 2018; Suaria and Aliani, 2014; van der Hal et al., 2017). Moreover, observational strategies are carried out by different teams using different techniques, so results are not always comparable. For these reasons, numerical modelling is needed to get insight in the mechanisms and patterns of ML dispersal in the Mediterranean.

Zambianchi et al. (2014) made a complete summary of the physical mechanism driving the ML dispersion in the Mediterranean basin and the scientific efforts carried out to analyze and understand this problem since the early 1980s. The concentrations of plastics estimated by the global models in the Mediterranean considerably differ from the observations, both in terms of quantified values at field and in the spatial distribution (Van Sebille et al., 2015). This is partially

due to the fact that the Mediterranean basin has its own thermohaline circulation, and a complex mesoscale field that includes fronts, filaments and eddies that the global models are not able to reproduce (Calafat et al., 2012; Millot, 1999; Poulain et al., 2012). Therefore, in this region it becomes mandatory to use high resolution regional models that are able to resolve those processes to accurately reproduce the circulation of the basin (Beuvier et al., 2012, 2010; Escudier et al., 2016; Herrmann et al., 2008; Sannino et al., 2015).

In recent years, few modeling studies on the concentration of marine litter in the Mediterranean have been carried out, primarily implementing lagrangian models of particle dispersion based on current fields obtained from regional high resolution circulation models. These works include those analyzing the whole basin (Liubartseva et al., 2018; Macias et al., 2019; Mansui et al., 2015) and also specific regions such as the Adriatic, Ligurian, Tyrrhenian or Aegean seas (Fossi et al., 2017; Liubartseva et al., 2016; Palatinus et al., 2019; Politikos et al., 2017). Zambianchi et al. (2017) followed a different approach, using a large database of lagrangian drifters over the basin to infer the probability of dispersion between adjacent regions, thus not using any numerical model. The results of all those studies are disparate, and highlight the difficulty of a task jeopardized by the lack of accurate information on the sources and total amount of marine litter that is discharged into the basin. In this sense, Liubartseva et al. (2018) is the only work to date that tries to make a realistic approximation of ML distribution for the entire basin, considering different sources (population centers, river discharge and maritime traffic). Additionally, it is worth commenting that most studies only focus on the modelling of floating particles, which is only a fraction of the total amount of ML released into the sea. A large fraction of polymers used to manufacture the more commons plastics items are denser than the average sea water (GESAMP, 2019). Therefore, it is expected that a large fraction of ML will not remain at the surface. In fact, several studies focused on the measurement of sedimented ML have found important amounts of marine litter in the seafloor of the basin at different depths from coastal to offshore seafloor habitats under different

human pressures (Alomar et al., 2016; García-Rivera et al., 2017; Ioakeimidis et al., 2014; Pham et al., 2014; Sanchez-vidal et al., 2018). Furthermore, there is also a significant fraction of polymers with densities within the range of the seawater density, thus behaving as neutral particles subject to the vertical currents. These particles can move along the whole water column and, particularly, along the photic layer, where most marine organisms live (Ventero et al., 2019). Only Liubartseva et al. (2018) consider the sedimentation process, although not explicitly resolving the vertical displacement of the particles but using a statistical approach. Consequently, plastics within a wide range of densities are present from the sea surface to the seafloor in marine environments being available for marine biota with different ecological habits (Deudero and Alomar, 2015). Given that many organisms present daily vertical migrations feeding in the photic layer, it is important to study ML vertical distribution, integrating a wide range of the feeding habitat of species which are susceptible to plastic ingestion (Compa et al., 2019a; Rios-Fuster et al., 2019).

In this context, the objective of this work is to characterize the spatial and temporal variability of the 3D dispersion of ML in the Mediterranean Sea, using a realistic distribution of the input sources and high resolution ocean currents. For this aim, a lagrangian dispersion model is implemented using the current field obtained from a very high resolution regional circulation model. In contrast with previous works that only simulate floating particles on the sea surface, our modeling system solves the 3D motion of three types of particles (floating, neutrally buoyant and sinking). This will allow for the first time, an analysis of the vertical distribution of ML, which is very relevant from an ecological and biological perspective. The article is organized as follows. Section 2 describes the modeling system, the simulations and the data analysis methodology. The results of the different simulations are presented in section 3 and discussed in section 4. Finally, the main conclusions are summarized in section 5.

2. Methodology

2.1. Modeling system

The modeling system used is based on two components, a regional high resolution circulation model (RCM) reproducing the 3D current velocity field in the Mediterranean (NEMOMED36) and a lagrangian model that simulates the evolution of floating particles (Ichthyop 3.3).

Regional circulation model

The circulation model used to simulate the Mediterranean currents field is NEMOMED36. It is a very high resolution regional configuration of the core model NEMO, with 1/36 x 1/36 degrees resolution (~ 3 km), covering the period 2003 – 2013 with daily resolution (Arsouze et al., 2013). It has 50 stretched z-vertical levels (from Δz of 1 m at the surface and 460 m at the bottom) with partial step parameterization for the bottom level. The model is initialized with a 3D temperature and salinity climatology provided by MEDATLAS-II for the period 1958-1986. The boundary is only open on the west side since the model covers the whole Mediterranean Basin. Moreover, in the Atlantic there is a buffer zone where temperature and salinity are restored towards the climatology of Levitus et al. (2005). In addition, a damping of Sea Surface Height (SSH) is done in this area towards prescribed SSH, given by previous version of the model that assimilates satellite altimetry data, to ensure volume conservation. River runoff is simulated as a freshwater increase near the grid points where the river is supposed to be with values of the main rivers obtained from RivDis database (Ludwig et al., 2009). The Black Sea is considered a river with its entrance at the Dardanelles Strait. The model is forced by ARPERA (Herrmann and Somot, 2008), a dynamical downscaling done by spectral nudging using the atmospheric model ARPEGE-Climate; Déqué and Piedelievre 1995), where scales above 250 km are spectrally driven by ECMWF fields (https://climatedataguide.ucar.edu/climate-data/era40) and small scales are allowed to freely develop. Several work using NEMOMED36 and previous versions have proven its ability to properly reproduce the main characteristics of the basin circulation, including

complex processes such as the deep water formation in the Eastern Mediterranean Transient (Beuvier et al., 2010) or the deep water formation at the Gulf of Lions (Beuvier et al., 2012).

Lagrangian model

The Ichthyop 3.3 model is an Individual Based Model (IBM) designed to study the effects of physical factors on the dynamics of fish eggs and larvae (Lett et al., 2008) (available at http://www.ichthyop.org/). It uses an eulerian model velocity field to infer the 3D particles trajectories resolving the movement equations through a fourth order Runge – Kutta integration scheme. The advective velocities from the eulerian model (U,V,W) are tri-linearly interpolated in space and linearly interpolated in time to the position of the particles. Then the particle evolution is estimated using the following equations:

$$\Delta x(x,y,z,t) = U(x,y,z,t)\Delta t + u_r \quad (1)$$

$$\Delta y(x,y,z,t) = V(x,y,z,t)\Delta t + v_r \quad (2)$$

$$\Delta z(x,y,z,t) = W(x,y,z,t)\Delta t \quad (3)$$

where Δx, Δy and Δz are the particle displacement after a time step Δt. The effect of the horizontal diffusivity is included by adding a random component to the horizontal velocities, u_r and v_r, estimated as:

$$(u,v)_r = \delta\sqrt{2K_{h_{x,y}}/\Delta t} \quad (4)$$

Here δ is a real uniform random number ($\delta \in$ [-1,1]), and K_h is the lagrangian horizontal diffusion imposed, of the form:

$$K_{h_{x,y}} = \varepsilon^{1/3} l_{x,y}^{4/3} \quad (5)$$

Where $l_{x,y}$ are the unresolved horizontal sub-grid scales (taken as the cell x and y sizes) and ε = 10^{-9} $m^2 \cdot s^{-3}$, is the turbulent dissipation rate (Peliz et al., 2007). Note that the vertical diffusivity is not considered in the computation of the vertical displacements.

In the boundaries and the coastal areas of the eulerian model domain, the particles behavior is set to "*bouncing"*, meaning that when the particle finds a coastal or a boundary pixel it bounces and moves back to the ocean part of the domain. Beaching effects have not been taken into account due to the existing uncertainties in the modelling of this process, especially with models that cannot explicitly reproduce the coastal boundary layer for which resolutions of o(10m) would be required. The integration time step is 15 minutes and daily outputs are stored. The Ichthyop model has been satisfactorily applied in physical and biological studies focused on pollutants transport (Millet et al., 2018), particle dispersions in harbor areas (Jouanneau et al., 2013), fisheries distribution (Džoić et al., 2017) and ecosystem connectivity (D'Agostini et al., 2015).

2.2. Simulations

Neutral particles simulation

Following the previous work of Jambeck et al. (2015) and Liubartseva et al. (2018), we assume a total input of 100k tons of plastic per year into the whole Mediterranean Sea. This total amount is distributed in three different types of sources: cities, rivers and maritime traffic or ships - lanes, according to the ratio 50:30:20% respectively.

The 50k tons of plastic per year corresponding to the cities are redistributed in proportion to their population. The cities have been selected as those with a population higher than 25k inhabitants, according to The Database on City Population (http://www.citypopulation.de). A total of 480 coastal cities are considered, most of them located along the shores of Spain, France and Italy (fig. 1). The 30k tons per year of the rivers are distributed among the fifteen

main rivers of the basin in proportion to their mean discharge between 1980 and 2012, estimated by the OCHIDEE River Flow model (Ducharne et al., 2003). The Black Sea input is not considered because the plastic concentration that leaves the Black Sea through the Dardanelles Strait is not clear. Assuming that all plastic dumped into the Black Sea reaches the Aegean Sea leads to a large overestimation of concentrations in the Aegean Sea, while having no significant effect for the rest of the domain (figures not shown). The position of the coastal sources (cities and river mouths) is selected as the model ocean grid point closer to its actual location. The 20k tons corresponding to the shipping lanes are uniformly distributed over the regions where concentrations of higher maritime traffic are found (Marine Traffic, 2015). Figure 1 shows the position of the different sources.

The modelling period covers ten years, between 2003 and 2013. Due to computational limitations, it has been divided in 120 simulations, each one running one year and starting the first day of each month. The distribution of particles has been carried out according to the previous considerations. A total of 41872 particles are released every month, which for the complete experiment makes a total of more than 5 million particles. The initial concentrations at the different sources location are represented in figure 1.

It is important to point out that the particles released in this simulation are defined as neutral (NP hereinafter), which means that their density is exactly the same as the density of the seawater surrounding them. In consequence, their vertical movements only depend on the vertical velocities given by the circulation model. Therefore, this simulation should be interpreted as an experiment describing the evolution of the fraction of ML that (a) behaves like neutral particles either because of their density or their shape and (b) reaches the open sea (i.e. not retained in the coastal area). Unfortunately, there are no estimates of what fraction of the total ML release falls in these two categories. In order to give dimensional concentration maps we assume that all the 100k released per year reach the open sea and have neutral density.

Nevertheless, due to the uncertainties on the actual amount of plastic that reaches the open sea, the absolute value of the concentrations should be taken with caution, and rather focus on the relative differences among regions or simulations.

Figure 1. Spatial distribution of initial marine litter concentrations (in kg/km^2) for the three simulations. Circle filled points indicate cities, diamonds indicate rivers and points over the sea indicate the ship lines.

Floating and sinking particles simulations

The effect of the density of the ML particles in their evolution along the basin has been analyzed by carrying out two complementary simulations using floating and sinking particles (referred as FP and SP hereinafter). The objective of these simulations is to analyze dispersion of these ML particles to assess how the density of the particles modify their spread across the basin and consequently their availability for marine biota.

The set-up of these experiments is similar to that of the experiment with neutral particles. The same number of particles are released using the same ML sources distribution and over the same time period. The difference is that in these runs the vertical motion of the particles is constraint. For the floating particles, vertical velocities are set to zero, so they are restricted to the surface layer. For the sinking particles, a nominal sedimentation velocity of the particles of -10^{-3} m/s is considered. It has to be noted that this sedimentation velocity is lower than the those obtained in laboratory experiments for particles with densities slightly higher than the water density (Khatmullina and Isachenko, 2017). These authors estimated sinking velocities between 0.005 and 0.127 m/s for items in the density range of 1130 – 1168 kg/m^3. We have selected a sedimentation velocity lower than the observed in laboratory in order establish an upper limit for the horizontal dispersion of sinking ML. In any case, this experiment should not be considered as an exhaustive representation of the ML sedimentation process, but as an approximation to the upper range of the possible evolution of the denser ML particles. In

summary, the three types of particles correspond to ML manufactured with polymers with densities lower than seawater (<1020 km/m^3, Floating particles), in the range of seawater (1020-1040 kg/m^3, Neutral particles) and denser than seawater (>1040 kg/m^3, Sinking particles. The main characteristics of the three experiments are summarized in table 1.

Simulation	Short name	Integration time	Vertical velocity
Neutral particles	S-NP	120 sim of 1yr	Given by the circulation model
Floating particles	S-FP	120 sim of 1yr	0
Sinking particles	S-SP	120 sim of 1yr	-10^{-3} m·s^{-1} added to the vertical velocity field from the circulation model

Table 1. Summary of the main characteristics of the three simulations analyzed.

2.3 Data analysis

The results of the numerical experiments have been processed to produce average ML concentration maps over the Mediterranean basin. These maps are computed by dividing the Mediterranean basin in a regular grid of 0.25º x 0.25º cells. The average concentration is estimated as the number of particles in each cell, divided by the cell surface, at each time step. Along with the concentration, the average depth of the particles at each grid cell is also computed.

For the neutral particles simulation, the concentration has been estimated in two separate depth layers: above and below the photic layer. The aim of this division is to analyze the fraction of the ML particles that will interact with pelagic organisms, whose distribution in depth is limited by light availability. The depth of the base of the photic layer has been obtained from SeaWifs satellite images. Monthly estimates downloaded from

https://oceandata.sci.gsfc.nasa.gov/SeaWiFS/Mapped/Monthly/9km/Zeu_lee/ have been averaged for the period 1997-2010 to obtain a 12-month climatology for the region. The average depth of the base of the photic layer ranges between 2 and 140 m depth.

3. Results

3.1 Average marine litter concentration

The maps of the averaged concentration for the neutral particles, above and below the base of the photic layer (BPL), the floating particles and the sinking particles are reproduced in figure 2. In the photic layer the average concentration of NP for the whole basin is 2.3 kg/km^2 (~80% of the total concentration). The regions of higher concentration in the Western Mediterranean are located in the Gulf of Lions and the northeastern slope of the Iberian Peninsula, with values reaching 6 kg/km^2 (fig. 2a). In this sub-basin, the regions with lower particle accumulation are located in the southern Tyrrhenian Sea (southeast of Sardinia), Ligurian and the Alboran Sea, with average concentrations lower than 1.5 kg/km^2. North of the Algerian current and in the Balearic Sea the average concentrations are moderate, with values between 2 and 4 kg/km^2. In the Eastern Mediterranean, the higher concentrations (>6.5 kg/km^2) are found in the proximities of the Sicily Strait and the Gulf of Gabes, the Adriatic Sea and the slopes of the Levantine basin from Egypt to Turkey. On the other hand, the northern Aegean, northern Ionian and center region of the Levantine basin show the lowest concentrations (< 1.5 kg/km^2). Throughout the rest of the Eastern Mediterranean, the concentrations range between 2 and 3 kg/km^2. The number of neutral particles found below the photic layer is very small in comparison, lower than 20% for the whole Mediterranean except for a small region in the

Aegean (not shown) (note that the color scale in figure 2b is different for this layer). The concentration is lower than 1 kg/km^2 in the whole basin except in the Northern Current region, the southern Adriatic, the Aegean and the coasts of the Levantine basin. There are large areas of the Ionian and Tyrrhenian Seas where the concentration is practically zero below the base of the photic layer. The depth distribution of the particles will be examined with more detail in the following section.

The spatial distribution of the floating particles is very similar to those of the neutral particles inside the photic layer. The regions with higher/lower concentrations coincide (fig. 2c). The most significant difference is an increase of the average concentration in the central Western Mediterranean, particularly noticeable in the Balearic Sea where the concentration increases up to 3 kg/km^2 north of Minorca Island. Conversely, the results for the sinking particles are completely different from for the other two simulations (fig. 2d). Even though the sedimentation speed added to the particles is relatively small, the particles sink very quickly and most of them remain roughly at the same location where they were released. As a result, the average concentration map for the sedimented particles highly resembles the initial concentrations at these positions (Compare fig. 2d with fig. 1).

Figure 2. Average marine litter concentration for the three simulations: a) Neutral particles above the base of the photic layer. b) Neutral particles below the base of the photic layer. c) Floating particles. d) Sinking particles, the black thin line indicates the 400 m isobath. Units are kg/km^2. Note that the range of values in (b) is different.

An interesting point in the analysis is to determine the contribution of each of the pollution sources to the ML concentrations. Figure 3 depicts the contribution of each type of ML source (cities, rivers and ships) to the average concentration of neutrally buoyant particles. In the Western Mediterranean, the main contribution comes from city inputs, with values higher than 60% practically over the whole region (fig. 3a). The rivers contribute to less than 20% and is

limited to the northwestern area of the sub-basin (except for a small region close to the Rhone mouth, where it reaches 60%) (fig. 3b). The contribution from the shipping lanes is also lower than 30% and is rather uniform throughout the whole sub-basin (fig. 3c). In the Eastern Mediterranean, the contribution from the cities, although still the most important, only exceeds 50% in the proximity of the Strait of Sicily, the Gulf of Gabes and the northern Aegean (fig. 3a). In this sub-basin the large Nile and Po rivers inputs contributes with more than 50% in the slope of the Levantine basin and the Adriatic Sea, respectively (fig. 3b). On the other hand, the contribution from shipping lanes in the Levantine basin and the Ionian Sea can reach 60% (fig. 3c). These are the areas that are less affected by the input of the other two sources, and hence where the average concentration is lower (fig. 2a).

Figure 3. Contribution of the three marine litter sources. a) cities, b) rivers and c) ships, to the averaged marine litter concentration showed in Figure 2a.

3.2 Temporal variability of ML concentration

In order to identify the areas of the basin with higher/lower temporal variability of ML concentration, the percentile maps of the daily values are computed for the neutral particles (fig. 4). The range of moderate variations is estimated using the interquartile range (p75th – p25th), which characterizes the range of values that are obtained at a certain location 50% of the time (Fig 4a). The results show that the regions with the highest variability are those with the highest average concentrations (i.e. compare with fig. 2): The Northern Current area, Gulf of Gabes, Adriatic Sea and the northeastern coast of the Levantine basin. In these regions, the interquartile range is almost of the same magnitude as the average value and variations of the order of 4 – 5 kg/km^2 are expected (fig. 4a). In addition, the regions with very strong variability can be identified by the extreme percentiles (p5th, and p95th, fig. 4b, c, respectively). For instance, in the central Western Mediterranean, the Adriatic or the Southern Aegean Seas, we can find minimum values below 1 kg/km^2 and maximum values above 6 kg/km^2. On the other

hand, in the southern Tyrrhenian, northern Ionian and northern Aegean the lowest variability is observed, where the concentration range between 0.5 and 2.5 kg/km^2.

Figure 4. Quantiles of the marine litter concentration. **a)** Interquartile range (p75th – p25th), **b)** p05th and **c)** p95th.

Regarding the time variability, it is also interesting to analyze if there is a significant seasonal cycle in the variability of the ML concentration in different regions of the Mediterranean. Of course, for the whole basin the number of particles is constant as the particles are not allowed to leave the basin and we have not considered any seasonality in the particles input from the different sources. Thus, the seasonal variability in our simulations is only the result of the seasonality of the current fields.

The spatially averaged seasonal cycles of the neutral and floating particles concentration for the main sub – basins of the Mediterranean are represented in figure 5. In general, the shape of the cycle for the FP and NP is very close, with larger amplitudes for the former due to the higher variability of the surface currents (not shown). For this reason, the analysis focuses on the FP hereinafter. The seasonal variability in the whole Eastern and Western sub-basins is negligible (fig. 5). That is, the amount of particles moving from one basin to the other is very small. Conversely, in the smaller sub-basins a clear seasonality is found due to the seasonality of the current filed. In the Western Mediterranean, a marked seasonal cycle is observed in the Balearic Sea, with an amplitude of 1.9 kg/km^2 peaking in August and with its minimum in February, and in the Gulf of Lions, with an amplitude of 1.2 kg·km^{-2} peaking in February and with its minimum July. For the Tyrrhenian Sea the seasonality is very low, with an amplitude lower than 0.5 kg·km^{-2} peaking in May and its minimum in October. In the Eastern basin, the Adriatic and Aegean Seas show significant seasonality, with similar amplitudes of 1.4 kg·km^{-2}. In the two regions the particle concentration reaches its maximum in late spring (April – May) and its minimum between late summer and fall (August – September). Conversely, in the Ionian Sea

and the Levantine basin the amplitudes are lower than 0.4 kg·km^{-2} and the cycle is of opposite phase, with maximum in late summer and minimum in spring.

Figure 5. Seasonal cycles of the ML concentration in the different sub-basins: Eastern Mediterranean (EMed, dark blue), Western Mediterranean (WMed, red), Levantine Basin (Lev, purple), Ionian Sea (ion, light blue), Aegean Sea (Aeg, cyan), Adriatic Sea (Adr, green), Tyrrhenian Sea (Tyrr, orange), Gulf of Lions (GoL, yellow) and Balearic Sea (Bal, salmon).

3.3 Vertical distribution of the particles.

Figure 6 shows the maps of average depth for the ML with neutral buoyancy. The mean depth across the whole basin is 22 m. In the Western Mediterranean the depth distribution is quite homogeneous, with values close to the whole basin average [20 – 30 m] (fig. 6). In the Eastern Mediterranean the mean depth distribution is more heterogeneous with regions as the southern Aegean, offshore the slope of the Gulf of Gabes and some areas of the Ionian Sea and the Levantine basin where the average depth reaches values higher than 45 m. Below the BPL the number of NP is very small (less than 10% of the total, not shown) and their depth distribution is very variable. The average depth is 177 m, but could reach up to more than 200 m in the north of the Balearic Islands, the Adriatic and the Aegean Sea. For the sinking particles the average depth map basically reproduces the model bathymetry at the position of the ML sources. As commented in the previous section, these particles quickly sink and reach the bottom with almost no time to be dispersed by the horizontal currents (fig. 2d). In consequence, the fraction of ML coming from cities and rivers that is denser than seawater sinks close to the coast, at depths lower than 400 m for the whole basin (see isobaths in fig. 2d).

Figure 6. Average of the vertical distribution of neutral particles (in meters (m)).

A more detailed description of the neutral particles depth distribution is obtained by analyzing the histograms in different regions (fig. 7). They represent the frequencies of the neutrally buoyant particles average depths in different regions of the Mediterranean basin. It should be recalled that the particles have neutral density and are released at the sea surface, so its vertical location is the result of the vertical motion of the water parcels.

The average depth of the NP for the whole basin is 35 m but a large number of them can be found above and below this depth (fig. 7a). Throughout most of the Western Mediterranean, the ML depth rarely exceeds 60 m (figs. 7c, h), and only in the Gulf of Lions a significant amount of particles reaches depths above 70 m (figs. 7i). In comparison, a large amount of particles reaches depths deeper than 60 m in the Eastern Mediterranean (fig. 7b). In the Adriatic and the Levantine basin a large number of particles can be found between 50 and 80 m (figs. 7d, g) while in the Aegean Sea most particles are located below 70 m depth, with a significant fraction reaching more than 100 m depth (fig. 7f). The exception is the Ionian Sea region, where most particles remain in shallower depths (< 40 m). In light of these results, it is clear that marine litter with a density range equal to the seawater density will not remain at the surface, but transported by the currents to the sea interior to depths ranging from 0 to 120 m.

For the interpretation of these results, it should be taken into account that figures 6 and 7 represent the average depth of the particles at each 0.25º x 0.25º bins. The fact that most particles remain near the surface limits the average value, but there is a small fraction of particles that sink to deeper depths (for clarity this has not been shown in the histograms). However, is important to remember that, due to limitations in the computational resources, the integration period of each simulation is one year, which limits the depths reached by the particles. One year is not enough time to allow the particles to spread along the whole water column. The stratification of the basin, where the ventilation of the intermediate and deep layers only takes place in very specific regions, also limits the capacity of the NP to reach deeper

layers. It is also relevant to point out that, as described in section 2.1, the lagrangian model does not include the effect of the vertical turbulent diffusivity in the computation of the vertical displacements, only the advective term derived from the eulerian current field is considered. Therefore, the effect of the vertical diffusion in the particles' vertical transport is neglected, but it is assumed that this would have a significant effect on time scales much longer than those considered here. Moreover, despite these limitations, the objective of the experiment with NP is to show that this fraction of marine litter extends all aver the basin along the photic layer very fast (in less than one year), and not only over the surface, building on previous modelling methodologies which have so far only considered the sea surface fraction.

Figure 7. Histograms of the average depth distribution of particles in the different sub-basins. a) Mediterranean Sea, b) Eastern Mediterranean, c) Western Mediterranean, d) Levantine Basin, e) Ionian Sea, f) Aegean Sea, g) Adriatic Sea, h) Tyrrhenian Sea and i) Gulf of Lions. For clarity, only the first 120 m are shown as far as the contribution below is very small.

4. Discussion

4.1. Concentration/dispersion areas in the Mediterranean basin

The results exposed in section 3.1 show that in most parts of the Western Mediterranean, and especially along the Catalan Coast, Balearic Sea and the Gulf of Lions, the ML concentration is very high due to the combination of the surrounding large cities and, to a lesser extent, the pollution coming from the Rhone and Ebro rivers (fig. 2, 3). In the Eastern basin, the accumulation areas are the Adriatic, the surroundings of the Strait of Sicily and the Gulf of Gabes, and the coastal area of the Levantine basin from Egypt to Turkey. In this case, in addition to the cities input, a large fraction of the ML contribution comes from the rivers Nile and Po (fig. 3). On the other hand, the dispersion areas (i.e. areas with lower than average concentrations) in the Western Mediterranean are found in the Alboran, Ligurian and Tyrrhenian seas. In the Eastern basin, the central part of the Levantine basin and the Northern Ionian Sea are the areas

with lower concentrations. These results are similar for the simulations using neutral and floating particles although for the latter the concentration in the surface of the Balearic Sea, Strait of Sicily and Gulf of Gabes are higher than for neutral particles (fig. 2a, c).

Previous studies based on global models show disparity in the identification of concentration/dispersion zones in the Mediterranean. Lebreton et al. (2012) point to the Ionian Sea and Levantine basin as the regions with higher concentration while Maximenko et al. (2012) obtained higher values in the Western Mediterranean. In Van Sebille et al. (2015), their simulation showed high ML concentrations over practically the whole Mediterranean, with the exception of the Tyrrhenian Sea. It must be noted that all these studies define very wide accumulation regions in the Mediterranean Sea as a direct consequence of the coarse resolution of the global models used. In fact, it is well stablished in the modeling community that, due to the complexity of the Mediterranean thermohaline circulation and the importance of the mesoscale activity in the basin, to accurately resolve the basin circulation high resolution ocean climate models are needed (Li et al., 2012; Somot et al., 2008), forced by high resolution atmospheric forcing (Herrmann and Somot, 2008) and taking into consideration river evolution (Skliris and Lascaratos 2004, Adloff et al. 2015). For this reason, the results based on global simulations, unable to resolve the basin mesoscale field, are most likely inaccurate in their description of the accumulation/dispersion regions of the basin.

Up until now, and to our knowledge, there are only three previous studies that have dealt with the simulation of ML dispersion across the whole basin using regional circulation models specifically adapted to the Mediterranean, and one work that used a velocity field derived from lagrangian drifters data. Mansui et al. (2015) performed a 1 – year simulations repeated every day and covering the period 2001 – 2010, all starting from a homogeneous ML distribution over the basin. The authors found four main accumulation zones: the central Western Mediterranean, the Tyrrhenian Sea, the Adriatic Sea and the southeast Ionian Sea. Similarly,

Macias et al. (2019) carried out a 18 – year long simulation also starting from a homogenous ML distribution. Their results show a different pattern with two main accumulation areas located in the eastern Ionian Sea and the central Levantine basin. Zambianchi et al. (2017) also started from a homogeneous distribution of passive tracers over the whole basin, identifying a main accumulation zone also in the central and coastal regions of the Levantine basin. The discrepancies of those studies with our work could be due to the initial distribution of particles. Therefore, in order to compare our results with them, a new simulation was carried out starting from a homogeneous distribution of floating particles over the whole Mediterranean (1 particle every three model grid points; a total of 47942 particles in each run). The temporal coverage is the same as for the rest of the simulations (120 simulations running one year and starting the first day of each month, between 2003 and 2012). The spatial distribution of the average concentration for this simulation is showed in figure 8. Similar to Mansui et al. (2015), we also find high concentration areas in the southwest Ionian, Adriatic and Tyrrhenian seas. Moderately high concentrations are also found in the northeastern Ionian, in agreement with Macias et al. (2019). On the contrary, the accumulation areas over the central Levantine basin (Macias et al., 2019; Zambianchi et al., 2017) and the central Western Mediterranean (Mansui et al. 2015) are not present. Conversely, high concentrations are found in the easternmost slope of the Levantine basin, the Aegean Sea and the northern current, which are not present in Mansui et al. (2015) and Macias et al. (2019), but agrees with the findings of Zambianchi et al. (2017) in the slope of the Levantine basin. As the starting point of the four simulations is the same one, the observed differences can be attributed to the differences in the representation of the current field used on the four studies. Mansui et al. (2015) used a lower resolution version (~9x9 km) of the NEMOMED RCM (NEMOMED12), with similar configuration and forcing than NEMOMED36. Macias et al. (2019) used a configuration the GETM model also with lower resolution (~9x9 km) but with a different parameterization and atmospheric forcing than NEMOMED12/36. Zambianchi et al (2017) derived the velocity field from the analysis of a large

dataset of drifters released all over the Mediterranean basin during the period 1985 – 2014. The density of the drifters is far from homogeneous, with most of them concentrated in the northern half of the basin, and very low densities in the Ionian and Levantine sub-basins. The comparison with the two studies based on numerical models current fields shows that our results are closer to those of Mansui et al. (2015), meaning that the RCM and the atmospheric forcing plays a very significant role in the final spatial distribution of the particles. On the other hand, the higher resolution of our model is the main difference with respect to the model used by Mansui et al. (2015), and our results are in better agreement with Zambianchi et al. (2017), in which the velocity field is derived from observations. This highlights the improvements achieved by increasing the model horizontal resolution.

Additionally, if we compare our results for S-FP simulation (fig. 2c) with the ones obtained starting from a homogeneous distribution (fig. 8) we also see significant differences. In particular, the concentrations in the eastern basin and in the Tyrrhenian Sea are much larger than in the later, while the concentrations over the continental shelf are larger starting the simulation with realistic sources of ML.

Figure 8. Average concentration for the simulation starting from a homogeneous particle distribution over the whole basin. Units are kg/km^2.

Liubartseva et al. (2018) carried out a 4.5 – year simulation analogous to S-FP of this study, starting with a realistic ML distribution but also including beaching and sedimentation processes in the particles evolution. These two processes remove particles from the simulation and are essential to understand the differences between their results and ours. In their work the authors estimate a half-life of the plastic particles between 7 and 80 days depending on the location of the source. It is important to differentiate the sedimentation mechanisms implemented in Liubartseva et al. (2018) from the simulation with sinking particles analyzed in this study. The authors simulate the sedimentation using a Monte Carlo algorithm that removes

particles from the surface by defining a probability of sedimentation that is proportional to the time. This way, the longer the time a particle is in the water, the most likely it will sediment, but not all the particles reach the seafloor. In other words, they analyze how the "age" of the particles leads to sedimentation by increasing its density (e.g. by biofouling), but the heavy particles that would sink almost immediately after entering the sea are not considered, so their results cannot be compared to our run with sinking particles. Comparing the other two simulations with the results from Liubartseva et al. (2018) we find that the results for the Western Mediterranean are in good agreement, with higher concentrations in the Catalan Coast, moderate in the central area of the sub – basin and lower in the Tyrrhenian Sea. For the Eastern Mediterranean more discrepancies are found. Both simulations agree in finding accumulation zones in the North Adriatic and North of Cyprus, but Liubartseva et al. (2018) also find an area of relatively high concentration in the central Ionian Sea that is not present in our simulation. Furthermore, their results show very low concentrations in the Aegean Sea in contrast with our estimates.

The seasonality of ML distribution was only previously analyzed by Macias et al. (2019). They found that particles concentrated more in the central months of the year (April – August), especially in the Balearic Sea, the Gulf of Gabes and the Nile mouth area, where values can double the mean concentration. In our case we do not find such big changes and seasonality only represents, at most, a 16% of the mean value. The same applies to our simulation starting from a homogeneous particle distribution (not shown).

In order to analyze the origin of the seasonality found in the simulations, Figure 9 shows the intensity of the NEMOMED36 velocity field averaged for the summer (JJA) and winter (JFM) months. The seasonal variability of the currents intensity over the basin can be used to explain the seasonality of the particles concentration. For instance, we can see that the northern current is stronger during winter and weakens in summer. Less intense currents allow a larger

fraction of particles to detach from the high concentration areas along the French and Iberian slopes and to travel towards the Balearic Sea. In consequence the concentration in summer increases in the Balearic basin while decreasing in the Gulf of Lions. We can also see that the intensity of the currents in the Adriatic and Aegean seas is higher in summer (fig. 9). This could explain the minimum in the seasonal cycle reached there in August – September (fig. 5). Stronger currents likely favors the transport of particles from these relatively enclosed regions towards the adjacent Ionian Sea and Levantine basin. Conversely, the cycles in these two regions are in opposite phase, as they are receiving the particles coming from the Adriatic and the Aegean.

Figure 9. Model average current intensity for a) summer and b) winter months. Units are m/s^{-1}

4.2 Vertical distribution of the ML

One of the main novelties of this study is that, for the first time, the dispersion of marine debris in the Mediterranean has been analyzed using a 3D approach that allows the description of the vertical distribution of the ML particles according to their density. The composition of the most commonly used plastic items includes polymers with densities lower (i.e. plastic bags or bottles caps), similar (i.e. fishing nets, ropes or textiles) and higher (i.e. bottles or cigarette filters) than that of seawater (GESAMP, 2019). Our results show that the particles with densities higher than seawater rapidly sink and reach the seafloor near their sources (figs. 2d). Therefore, the ML concentration at the bottom is directly dependent on the inputs from the different sources. This is consistent with recent observations of ML in the seafloor (Spedicato et al., 2019). In the case of the particles with neutral density, our results show that the regions of higher/lower concentration of neutral and floating particles are basically the same ones. This is not surprising considering that most NP remain in the first 120 m, where the circulation patterns are very similar to those at the sea surface. In consequence the fraction of marine litter comprised by

polymers with densities close to the sea water density spread all over the Mediterranean following the same paths than the floating litter, but distributed across the water column. In fact, the analysis shows that most of them remain in the photic layer and only 20% reach depths below it along the 1-year periods of the simulations (fig.7). Furthermore, the averaged depth is 35 m, meaning that most of this type of plastics are out of range of the usual sampling mechanisms used in the observational campaigns (visual census and surface net trawling, i. e., manta trawls). This result is crucial to be considered if a quantification of the actual amount of plastics in the Mediterranean is needed. As stated in the introduction, many authors have studied the interaction of macro and micro plastics with a broad diversity of marine species and most studies of marine litter distribution are limited to the surface, where only a fraction of all plastics will remain. In consequence, it is expected that the actual concentrations of plastics in the sea will be much larger than the values estimated from surface observations.

4.3 Concentration variability and sampling strategies

The description of ML dispersion using numerical simulations has two main limitations: the accuracy of the RCM to properly resolve the basin circulation and the definition of the initial concentrations of the different sources. In the first case, although far from being perfect, regional circulation models have proven their skills to satisfactorily reproduce complex processes of the Mediterranean circulation (Herrmann et al., 2008; Beuvier et al., 2012, 2010; Sannino et al., 2015; Soto-Navarro et al., 2015; Escudier et al., 2016). In the case of the initial particle concentrations, the actual amount of plastics that ends-up in the open sea is still unknown. All of the studies trying to use realistic ML inputs base their initial concentration on indirect estimations. In our case and in the study of Liubartseva et al. (2018), the initial concentrations are based on the work of Jambeck et al. (2015). These authors infer the amount of plastic entering the ocean by analyzing socio-economic indicators of the production, use and management of plastic items. As a consequence, the initial conditions of the simulations are

subject to large uncertainties, so a direct comparison with observations can be challenging. In other words, trying to match observations obtained in a given date is challenging if no information is available about the concentrations of the previous days/weeks to initialize the model. Nevertheless, the model results provide useful information about the average patterns (i.e. climatological-type fields), and the expected temporal variability of ML concentrations. In turn, this information could explain the large scattering of observed values reported in the literature.

A good example is the effect of the seasonality of the ML concentration in the results of the measuring campaigns. One of the main bias present in the studies of ML distribution based on observations is that most of them collect their samples only in the spring-summer months, when the meteorological conditions are favorable. As previously discussed, in some regions there is a considerable seasonality in the ML concentration derived from the current field variability. For instance, in the Balearic Sea the concentrations are higher in summer, what could have influenced the results of several works that find high levels of ML concentration sampling in that region between May and October (Compa et al., 2019b; Cózar et al., 2015; Ruiz-Orejón et al., 2016; Suaria et al., 2016; Suaria and Aliani, 2014). As previously commented, the simulations only consider the variability resulting from the evolution of the current field. Changes of the ML distribution derived from the variability in the inputs from the sources are not included and could largely affect the observed concentrations (Arcangeli et al., 2018; Baini et al., 2018; Compa et al., 2019b).

With respect to the spatial distribution, strong differences are also found between the different observational studies. For instance, Cozar et al. (2015), Suaria and Aliani (2014) and Suaria et al. (2016) found very small concentrations in the south Adriatic and the Tyrrhenian Sea (in agreement with our results) while Arcangeli et al. (2018) found high values over these regions during the same periods. In the Eastern Mediterranean, the relatively low values found by Cozar

et al. (2015) in the Ionian Sea also coincide with our model estimation, while the higher values observed in the Levantine basin disagree with the simulations results. In addition, the spatial patterns observed in most studies are very noisy, with large differences between very close observation points and among studies. This could be explained by a sampling difficulties linked to the high temporal variability of ML concentration. In other words, the simulations suggest that time variability of ML concentration can be very high. Thus, the observational results are strongly dependent on the exact time the observations where obtained.

Taking into account all the previous considerations, the variability of the particle concentration summarized in figures 4 and 5 can be used to identify the regions and time periods where/when higher/lower values are expected and use that information in the design of sampling strategies. For instance, the Balearic and Adriatic Seas can be considered highly variable regions, where the average concentrations are relatively high and show strong variability. In these areas the ML observations will drastically change depending on the time of the year in which the campaign is carried out. An adequate sampling strategy should include measures throughout the whole year, or, at least, during the months where the seasonal cycle reaches its maximum and minimum. By doing this the seasonal bias would be reduced and the observations would be more representative of the actual concentration along the year. In other regions, like the northern Ionian, southern Tyrrhenian or the Ligurian Sea, the variability and seasonality are relatively low (fig. 4, 5). Therefore, the result of summer/winter campaigns would not be largely affected by the current field variability.

In addition, the sampling strategies should also consider the vertical distribution of the neutral particles discussed in the previous section. In order to understand how marine plastic interacts with the different Mediterranean ecosystems it is necessary to assess its presence throughout the water column, and especially within the photic layer.

5. Conclusions

The dispersion of marine litter particles over the Mediterranean basin have been simulated using high resolution (2-3km) 3D current fields that have fed a lagrangian model. Three simulations have been carried out, all starting from a realistic initial distribution of ML sources, and covering a ten-year period (2003 – 2013). The evolution of particles with positive, neutral and negative buoyancy has been studied allowing, for the first time in the Mediterranean, the study of the vertical distribution of ML. The three types of particles correspond to ML manufactured with polymers with densities lower than seawater (<1020 km/m^3), in the range of seawater (1020-1040 kg/m^3) and denser than seawater (>1040 kg/m^3).

The results show that the accumulation/dispersion areas of the floating and neutral particles are very similar although in the latter the particles are distributed across the upper 120 m with an averaged depth of 35 m. The highest concentrations of neutral particles are found in the Catalan continental shelf, the proximities of the Strait of Sicily and the Gulf of Gabes, the Adriatic Sea and the easternmost slope of the Levantine basin. For the floating particles large concentrations are also found in the Balearic Sea. On the other hand, the particles with negative buoyancy rapidly sink and reach the seafloor close to their sources, with no time to disperse. The analysis of the temporal variability of the ML concentration due to the variability of the currents shows that the regions of higher variability mostly coincide with the accumulation regions.

The comparison among different studies suggests that the main limitation of the modeling studies is linked to the lack of accurate information about the amount of ML released into the sea from different sources. Additionally, there are several issues that could be explored in the future. One of them would be to include the effects of population fluctuation in the coastal areas due to, for instance, the touristic seasonality, as well as the seasonal variability of the river discharge. Another one would be to improve the model representation of the vertical displacements, through the inclusion of the vertical diffusivity and extending as much as

possible the integration time. In this way the vertical displacements of the NP will be more accurately represented and the particles will have enough time to spread along the whole water column, leading to a better estimate of the cumulative effects of ML in the deeper layers.

The results presented in this work can also be used in the design of field campaigns to study marine litter distribution. The sampling strategies should consider at least the seasonal variability of each region (i.e. by sampling in different seasons in places with strong seasonality). Also, if the campaign aims at a quantification of the total amount of plastics, measurements of the vertical distribution of the ML would also be necessary, in particular across the photic layer.

Acknowledgments

Acknowledgements to the EU-funded Interreg Med Plastic Busters MPAs project: preserving biodiversity from plastics in Mediterranean Marine Protected Areas, co-financed by the European Regional Development Fund. M. Compa is the recipient of an FPI Fellowship from Conselleria d'Innovació, Recerca I Turisme of the regional Government of the Balearic Islands co-financed by the European Social Fund as part of the FSE 2014–2020 operational program. We thank Dr. T. Arsouze and the SIMED project for providing the NEMOMED36 dataset. We also thank the two anonymous reviewers for their suggestions that help to improve the quality of this paper.

References

Aliani, S., Molcard, A., 2003. Hitch-hiking on floating marine debris: macrobenthic species in the Western Mediterranean Sea, in: Jones, M.B., Ingólfsson, A., Ólafsson, E., Helgason, G. V, Gunnarsson, K., Svavarsson, J. (Eds.), Migrations and Dispersal of Marine Organisms. Springer Netherlands, Dordrecht, pp. 59–67.

Alomar, C., Compa, M., Deudero, S., Guijarro, B., 2019. Spatial and temporal distribution of marine litter on the seafloor of the Balearic Islands (western Mediterranean Sea). Deep-

Sea Research Part I: Oceanographic Research Papers 103178. doi:10.1016/j.dsr.2019.103178

Alomar, C., Estarellas, F., Deudero, S., 2016. Microplastics in the Mediterranean Sea : Deposition in coastal shallow sediments , spatial variation and preferential grain size. Marine environmental … 115. doi:10.1016/j.marenvres.2016.01.005

Arcangeli, A., Campana, I., Angeletti, D., Atzori, F., Azzolin, M., Carosso, L., Di Miccoli, V., Giacoletti, A., Gregorietti, M., Luperini, C., Paraboschi, M., Pellegrino, G., Ramazio, M., Sarà, G., Crosti, R., 2018. Amount, composition, and spatial distribution of floating macro litter along fixed trans-border transects in the Mediterranean basin. Marine Pollution Bulletin 129, 545–554. doi:10.1016/j.marpolbul.2017.10.028

Arsouze, T., Beuvier, J., Béranger, K., Somot, S., Brossier, C.L., Sevault, F., Drillet, Y., 2013. Sensitivity Analysis of the Western Mediterranean Transition inferred by four companion simulations. Rapp. Comm. Int. Mer Médit. 32442. doi:10.1029/2008GL035146.2

Azzarello, M.Y., Van Vleet, E.S., 1987. Marine birds and plastic pollution. Marine Ecolgy - Progress Series 37, 295–303.

Baini, M., Fossi, M.C., Galli, M., Caliani, I., Campani, T., Finoia, M.G., Panti, C., 2018. Abundance and characterization of microplastics in the coastal waters of Tuscany (Italy): The application of the MSFD monitoring protocol in the Mediterranean Sea. Marine pollution bulletin 133, 543–552.

Barnes D. K., 2002. Biodiversity: Invasions by marine life on plastic debris. Nature 416, 808–809.

Barnes, D.K.A., Galgani, F., Thompson, R.C., Barlaz, M., 2009. Accumulation and fragmentation of plastic debris in global environments. Philosophical Transactions of the Royal Society B: Biological Sciences 364, 1985–1998. doi:10.1098/rstb.2008.0205

Baulch, S., Perry, C., 2014. Evaluating the impacts of marine debris on cetaceans. Marine Pollution Bulletin 80, 210–221. doi:10.1016/j.marpolbul.2013.12.050

Beuvier, J., Béranger, K., Brossier, C.L., Somot, S., Sevault, F., Drillet, Y., Bourdallé-Badie, R., Ferry, N., Lyard, F., 2012. Spreading of the Western Mediterranean Deep Water after winter 2005: Time scales and deep cyclone transport. Journal of Geophysical Research: Oceans 117. doi:10.1029/2011JC

Beuvier, J., Sevault, F., Herrmann, M., Kontoyiannis, H., Ludwig, W., Rixen, M., Stanev, E., Branger, K., Somot, S., 2010. Modeling the Mediterranean Sea interannual variability during 1961-2000: Focus on the Eastern Mediterranean Transient. Journal of Geophysical Research: Oceans 115. doi:10.1029/2009JC005950

Calafat, F.M., Jord, G., Marcos, M., Gomis, D., 2012. Comparison of Mediterranean sea level variability as given by three baroclinic models. Journal of Geophysical Research: Oceans 117, 1–23. doi:10.1029/2011JC007277

Carson, H.S., 2013. The incidence of plastic ingestion by fishes: From the prey's perspective. Marine Pollution Bulletin 74, 170–174. doi:10.1016/j.marpolbul.2013.07.008

Compa, M., Alomar, C., Wilcox, C., van Sebille, E., Lebreton, L., Hardesty, B.D., Deudero, S., 2019a. Risk assessment of plastic pollution on marine diversity in the Mediterranean Sea. Science of the Total Environment 678, 188–196. doi:10.1016/j.scitotenv.2019.04.355

Compa, M., March, D., Deudero, S., 2019b. Spatio-temporal monitoring of coastal floating marine debris in the Balearic Islands from sea-cleaning boats. Marine Pollution Bulletin 141, 205–214. doi:10.1016/j.marpolbul.2019.02.027

Cózar, A., Sanz-Martín, M., Martí, E., González-Gordillo, J.I., Ubeda, B., Gálvez, J.Á., Irigoien, X., Duarte, C.M., 2015. Plastic Accumulation in the Mediterranean Sea. Plos One 10,

e0121762. doi:10.1371/journal.pone.0121762

D'Agostini, A., Gherardi, D.F.M., Pezzi, L.P., 2015. Connectivity of marine protected areas and its relation with total kinetic energy. PLoS ONE 10, 1–19. doi:10.1371/journal.pone.0139601

Déqué, M., Piedelievre, J.P., 1995. High resolution climate simulation over Europe. Climate Dynamics 11, 321–339. doi:10.1007/BF00215735

Deudero, S., Alomar, C., 2015. Mediterranean marine biodiversity under threat: Reviewing influence of marine litter on species. Marine Pollution Bulletin 98, 58–68. doi:10.1016/j.marpolbul.2015.07.012

Ducharne, A., Golaz, C., Leblois, E., Laval, K., Polcher, J., Ledoux, E., De Marsily, G., 2003. Development of a high resolution runoff routing model, calibration and application to assess runoff from the LMD GCM. Journal of Hydrology 280, 207–228. doi:10.1016/S0022-1694(03)00230-0

Džoić, T., Beg Paklar, G., Grbec, B., Ivatek-Šahdan, S., Zorica, B., Šegvić-Bubić, T., Keč, V.Č., Pleić, I.L., Mladineo, I., Grubišić, L., Verley, P., 2017. Spillover of the Atlantic bluefin tuna offspring from cages in the Adriatic Sea: A multidisciplinary approach and assessment. PLoS ONE 12, 1–20. doi:10.1371/journal.pone.0188956

Eriksen, M., Lebreton, L.C.M., Carson, H.S., Thiel, M., Moore, C.J., Borerro, J.C., Galgani, F., Ryan, P.G., Reisser, J., 2014. Plastic Pollution in the World's Oceans: More than 5 Trillion Plastic Pieces Weighing over 250,000 Tons Afloat at Sea. PLoS ONE 9, 0–15. doi:10.1371/journal.pone.0111913

Escudier, R., Renault, L., Pascual, A., Brasseur, P., Chelton, D., Beuvier, J., 2016. Eddy properties in the Western Mediterranean Sea from satellite altimetry and a numerical simulation. Journal of Geophysical Research: Oceans 121, 3990–4006. doi:10.1002/2015JC011371

Faure, F., Saini, C., Potter, G., Galgani, F., de Alencastro, L.F., Hagmann, P., 2015. An evaluation of surface micro- and mesoplastic pollution in pelagic ecosystems of the Western Mediterranean Sea. Environmental Science and Pollution Research 22, 12190–12197. doi:10.1007/s11356-015-4453-3

Fossi, M.C., Romeo, T., Baini, M., Panti, C., Marsili, L., Campani, T., Canese, S., Galgani, F., Druon, J.-N., Airoldi, S., Taddei, S., Fattorini, M., Brandini, C., Lapucci, C., 2017. Plastic Debris Occurrence, Convergence Areas and Fin Whales Feeding Ground in the Mediterranean Marine Protected Area Pelagos Sanctuary: A Modeling Approach. Frontiers in Marine Science 4, 1–15. doi:10.3389/fmars.2017.00167

Gajšt, T., Bizjak, T., Palatinus, A., Liubartseva, S., Kržan, A., 2016. Sea surface microplastics in Slovenian part of the Northern Adriatic. Marine Pollution Bulletin 113, 392–399. doi:10.1016/j.marpolbul.2016.10.031

García-Rivera, S., Lizaso, J.L.S., Millán, J.M.B., 2017. Composition, spatial distribution and sources of macro-marine litter on the Gulf of Alicante seafloor (Spanish Mediterranean). Marine Pollution Bulletin 121, 249–259. doi:10.1016/j.marpolbul.2017.06.022

GESAMP, 2019. Guidelines for the monitoring and assessment of plastic litter in the ocean. GESAMP Reports & Studies 99, 130.

Herrmann, M., Estournel, C., Déqué, M., Marsaleix, P., Sevault, F., Somot, S., 2008. Dense water formation in the Gulf of Lions shelf: Impact of atmospheric interannual variability and climate change. Continental Shelf Research 28, 2092–2112. doi:10.1016/j.csr.2008.03.003

Herrmann, M.J., Somot, S., 2008. Relevance of ERA40 dynamical downscaling for modeling deep convection in the Mediterranean Sea. Geophysical Research Letters 35, 1–5. doi:10.1029/2007GL032442

Ioakeimidis, C., Zeri, C., Kaberi, H., Galatchi, M., Antoniadis, K., Streftaris, N., Galgani, F., Papathanassiou, E., Papatheodorou, G., 2014. A comparative study of marine litter on the seafloor of coastal areas in the Eastern Mediterranean and Black Seas. Marine Pollution Bulletin. doi:10.1016/j.marpolbul.2014.09.044

Jambeck, J. R., Gayer, R., Wilcox, C., Siegler, R.T., Perryman, M., Andrady, A., Narayan, R., Law, L.K., 2015. The ocean. Climate Change 2014: Impacts, Adaptation and Vulnerability: Part B: Regional Aspects: Working Group II Contribution to the Fifth Assessment Report of the Intergovernmental Panel on Climate Change 347, 1655–1734. doi:10.1017/CBO9781107415386.010

Jambeck, Jenna R, Geyer, R., Wilcox, C., Siegler, T.R., Perryman, M., Andrady, A., Narayan, R., Law, K.L., 2015. Plastic waste inputs from land into the ocean.

Jouanneau, N., Sentchev, A., Dumas, F., 2013. Numerical modelling of circulation and dispersion processes in Boulogne-sur-Mer harbour (Eastern English Channel): Sensitivity to physical forcing and harbour design. Ocean Dynamics 63, 1321–1340. doi:10.1007/s10236-013-0659-4

Khatmullina, L., Isachenko, I., 2017. Settling velocity of microplastic particles of regular shapes. Marine Pollution Bulletin 114, 871–880. doi:10.1016/j.marpolbul.2016.11.024

Koch, H.M., Calafat, A.M., 2009. Human body burdens of chemicals used in plastic manufacture. Philosophical Transactions of the Royal Society B: Biological Sciences 364, 2063–2078. doi:10.1098/rstb.2008.0208

Koelmans, A.A., Bakir, A., Burton, G.A., Janssen, C.R., 2016. Microplastic as a Vector for Chemicals in the Aquatic Environment: Critical Review and Model-Supported Reinterpretation of Empirical Studies. Environmental Science & Technology 50, 3315–3326. doi:10.1021/acs.est.5b06069

Law, K.L., Morét-Ferguson, S.E., Goodwin, D.S., Zettler, E.R., Deforce, E., Kukulka, T., Proskurowski, G., 2014. Distribution of surface plastic debris in the eastern pacific ocean from an 11-year data set. Environmental Science and Technology 48, 4732–4738. doi:10.1021/es4053076

Lazar, B., Gračan, R., 2011. Ingestion of marine debris by loggerhead sea turtles, Caretta caretta, in the Adriatic Sea. Marine Pollution Bulletin 62, 43–47. doi:10.1016/j.marpolbul.2010.09.013

Lebreton, L.C.M., Greer, S.D., Borrero, J.C., 2012. Numerical modelling of floating debris in the world's oceans. Marine Pollution Bulletin 64, 653–661. doi:10.1016/j.marpolbul.2011.10.027

Lett, C., Verley, P., Mullon, C., Parada, C., Brochier, T., Penven, P., Blanke, B., 2008. A Lagrangian tool for modelling ichthyoplankton dynamics. Environmental Modelling and Software 23, 1210–1214. doi:10.1016/j.envsoft.2008.02.005

Levitus, S., Antonov, J., Boyer, T., 2005. Warming of the world ocean, 1955-2003. Geophysical Research Letters 32, 1–4. doi:10.1029/2004GL021592

Li, L., Casado, A., Congedi, L., Dell'Aquila, A., Dubois, C., Elizalde, A., Hévéder, B.L., Lionello, P., Sevault, F., Somot, S., Ruti, P., Zampieri, M., 2012. 7 - Modeling of the Mediterranean Climate System, in: Lionello, P. (Ed.), The Climate of the Mediterranean Region. Elsevier, Oxford, pp. 419–448. doi:https://doi.org/10.1016/B978-0-12-416042-2.00007-0

Liubartseva, S., Coppini, G., Lecci, R., Clementi, E., 2018. Tracking plastics in the Mediterranean: 2D Lagrangian model. Marine Pollution Bulletin 129, 151–162. doi:10.1016/j.marpolbul.2018.02.019

Liubartseva, S., Coppini, G., Lecci, R., Creti, S., 2016. Regional approach to modeling the

transport of floating plastic debris in the Adriatic Sea. Marine Pollution Bulletin 103, 115–127. doi:10.1016/j.marpolbul.2015.12.031

Ludwig, W., Dumont, E., Meybeck, M., Heussner, S., 2009. River discharges of water and nutrients to the Mediterranean and Black Sea: Major drivers for ecosystem changes during past and future decades? Progress in Oceanography 80, 199–217. doi:10.1016/j.pocean.2009.02.001

Macias, D., Cózar, A., Garcia-Gorriz, E., González-Fernández, D., Stips, A., 2019. Surface water circulation develops seasonally changing patterns of floating litter accumulation in the Mediterranean Sea. A modelling approach. Marine Pollution Bulletin 149, 110619. doi:10.1016/j.marpolbul.2019.110619

Mansui, J., Molcard, A., Ourmières, Y., 2015. Modelling the transport and accumulation of floating marine debris in the Mediterranean basin. Marine Pollution Bulletin 91, 249–257. doi:10.1016/j.marpolbul.2014.11.037

Mato, Y., Isobe, T., Takada, H., Kanehiro, H., Ohtake, C., Kaminuma, T., 2001. Plastic resin pellets as a transport medium for toxic chemicals in the marine environment. Environmental Science and Technology 35, 318–324. doi:10.1021/es0010498

Maximenko, N., Corradi, P., Law, K.L., Van Sebille, E., Garaba, S.P., Lampitt, R.S., Galgani, F., Martinez-Vicente, V., Goddijn-Murphy, L., Veiga, J.M., Thompson, R.C., Maes, C., Moller, D., Löscher, C.R., Addamo, A.M., Lamson, M.R., Centurioni, L.R., Posth, N.R., Lumpkin, R., Vinci, M., Martins, A.M., Pieper, C.D., Isobe, A., Hanke, G., Edwards, M., Chubarenko, I.P., Rodriguez, E., Aliani, S., Arias, M., Asner, G.P., Brosich, A., Carlton, J.T., Chao, Y., Cook, A.-M., Cundy, A.B., Galloway, T.S., Giorgetti, A., Goni, G.J., Guichoux, Y., Haram, L.E., Hardesty, B.D., Holdsworth, N., Lebreton, L., Leslie, H.A., Macadam-Somer, I., Mace, T., Manuel, M., Marsh, R., Martinez, E., Mayor, D.J., Le Moigne, M., Molina Jack, M.E.,

Mowlem, M.C., Obbard, R.W., Pabortsava, K., Robberson, B., Rotaru, A.-E., Ruiz, G.M., Spedicato, M.T., Thiel, M., Turra, A., Wilcox, C., 2019. Toward the Integrated Marine Debris Observing System. Frontiers in Marine Science 6. doi:10.3389/fmars.2019.00447

Maximenko, N., Hafner, J., Niiler, P., 2012. Pathways of marine debris derived from trajectories of Lagrangian drifters. Marine Pollution Bulletin 65, 51–62. doi:10.1016/j.marpolbul.2011.04.016

Millet, B., Pinazo, C., Banaru, D., Pagès, R., Guiart, P., Pairaud, I., 2018. Unexpected spatial impact of treatment plant discharges induced by episodic hydrodynamic events: Modelling Lagrangian transport of fine particles by Northern current intrusions in the bays of marseille (France). PLoS ONE 13, 1–25. doi:10.1371/journal.pone.0195257

Millot, C., 1999. Circulation in the Western Mediterranean Sea. Journal of Marine Systems. doi:10.1016/S0924-7963(98)00078-5

Palatinus, A., Kovač Viršek, M., Robič, U., Grego, M., Bajt, O., Šiljić, J., Suaria, G., Liubartseva, S., Coppini, G., Peterlin, M., 2019. Marine litter in the Croatian part of the middle Adriatic Sea: Simultaneous assessment of floating and seabed macro and micro litter abundance and composition. Marine Pollution Bulletin 139, 427–439. doi:10.1016/j.marpolbul.2018.12.038

Peliz, A., Marchesiello, P., Dubert, J., Marta-Almeida, M., Roy, C., Queiroga, H., 2007. A study of crab larvae dispersal on the Western Iberian Shelf: Physical processes. Journal of Marine Systems 68, 215–236. doi:10.1016/j.jmarsys.2006.11.007

Pham, C.K., Ramirez-Llodra, E., Alt, C.H.S., Amaro, T., Bergmann, M., Canals, M., Company, J.B., Davies, J., Duineveld, G., Galgani, F., Howell, K.L., Huvenne, V. a I., Isidro, E., Jones, D.O.B., Lastras, G., Morato, T., Gomes-Pereira, J.N., Purser, A., Stewart, H., Tojeira, I., Tubau, X., Van Rooij, D., Tyler, P. a, 2014. Marine litter distribution and density in European seas,

from the shelves to deep basins. PloS one 9, e95839. doi:10.1371/journal.pone.0095839

Politikos, D. V., Ioakeimidis, C., Papatheodorou, G., Tsiaras, K., 2017. Modeling the Fate and Distribution of Floating Litter Particles in the Aegean Sea (E. Mediterranean). Frontiers in Marine Science 4, 1–18. doi:10.3389/fmars.2017.00191

Poulain, P.-M., Menna, M., Mauri, E., 2012. Surface Geostrophic Circulation of the Mediterranean Sea Derived from Drifter and Satellite Altimeter Data. Journal of Physical Oceanography 42, 973–990. doi:10.1175/JPO-D-11-0159.1

Rios-Fuster, B., Alomar, C., Compa, M., Guijarro, B., Deudero, S., 2019. Anthropogenic particles ingestion in fish species from two areas of the western Mediterranean Sea. Marine Pollution Bulletin 144, 325–333. doi:10.1016/j.marpolbul.2019.04.064

Ruiz-Orejón, L.F., Sardá, R., Ramis-Pujol, J., 2016. Floating plastic debris in the Central and Western Mediterranean Sea. Marine Environmental Research 120, 136–144. doi:10.1016/j.marenvres.2016.08.001

Ryan, P.G., Jackson, S., 1987. The lifespan of ingested plastic particles in seabirds and their effect on digestive efficiency. Marine Pollution Bulletin 18, 217–219. doi:10.1016/0025-326X(87)90461-9

Sanchez-vidal, A., Thompson, R.C., Canals, M., Haan, W.P. De, 2018. The imprint of microfibres in southern European deep seas 1–12.

Sannino, G., Carillo, A., Pisacane, G., Naranjo, C., 2015. On the relevance of tidal forcing in modelling the Mediterranean thermohaline circulation. Progress in Oceanography 134, 304–329. doi:10.1016/j.pocean.2015.03.002

Schmidt, N., Thibault, D., Galgani, F., Paluselli, A., Sempéré, R., 2018. Occurrence of microplastics in surface waters of the Gulf of Lion (NW Mediterranean Sea). Progress in

Oceanography 163, 214–220. doi:10.1016/j.pocean.2017.11.010

Skliris, N., Lascaratos, A., 2004. Impacts of the Nile River damming on the thermohaline circulation and water mass characteristics of the Mediterranean Sea. Journal of Marine Systems 52, 121–143. doi:10.1016/j.jmarsys.2004.02.005

Somot, S., Sevault, F., Déqué, M., Crépon, M., 2008. 21st century climate change scenario for the Mediterranean using a coupled atmosphere-ocean regional climate model. Global and Planetary Change 63, 112–126. doi:10.1016/j.gloplacha.2007.10.003

Soto-Navarro, J., Somot, S., Sevault, F., Beuvier, J., Criado-Aldeanueva, F., García-Lafuente, J., Béranger, K., 2015. Evaluation of regional ocean circulation models for the Mediterranean Sea at the Strait of Gibraltar: volume transport and thermohaline properties of the outflow. Climate Dynamics 44, 1277–1292. doi:10.1007/s00382-014-2179-4

Spedicato, M.T., Zupa, W., Carbonara, P., Fiorentino, F., Follesa, M.C., Galgani, F., García-Ruiz, C., Jadaud, A., Ioakeimidis, C., Lazarakis, G., Lembo, G., Mandic, M., Maiorano, P., Sartini, M., Serena, F., Cau, A., Esteban, A., Isajlovic, I., Micallef, R., Thasitis, I., 2019. Spatial distribution of marine macro-litter on the seafloor in the northern mediterranean sea: The MEDITS initiative. Scientia Marina 83, 257–270. doi:10.3989/scimar.04987.14A

Suaria, G., Aliani, S., 2014. Floating debris in the Mediterranean Sea. Marine Pollution Bulletin 86, 494–504. doi:10.1016/j.marpolbul.2014.06.025

Suaria, G., Avio, C.G., Mineo, A., Lattin, G.L., Magaldi, M.G., Belmonte, G., Moore, C.J., Regoli, F., Aliani, S., 2016. The Mediterranean Plastic Soup : synthetic polymers in Mediterranean surface waters. Nature Publishing Group 1–10. doi:10.1038/srep37551

UNEP, 2009*, Marine Litter A Global Challenge, Nairobi: UNEP. 232 pp.*

UNEP/MAO, 2015. Marine Litter Assessment in the Mediterranean 2015, ISBN No: 978-92-807-

3564-2

van der Hal, N., Ariel, A., Angel, D.L., 2017. Exceptionally high abundances of microplastics in the oligotrophic Israeli Mediterranean coastal waters. Marine Pollution Bulletin 116, 151–155. doi:10.1016/j.marpolbul.2016.12.052

Van Sebille, E., Chris, W., Laurent, L., Nikolai, M., Britta Denise, H., Jan, A. van F., Marcus, E., David, S., Francois, G., Kara Lavender, L., 2015. A global inventory of small floating plastic debris. Environmental Research Letters 10, 124006.

Ventero, A., IGLESIAS, M., CÓRDOBA, P., 2019. Krill spatial distribution in the Spanish Mediterranean Sea in summer time 00, 1–15. doi:10.1093/plankt/fbz030

Zambianchi, E., Iermano, I., Suaria, G., Aliani, S., 2014. Marine litter in the Mediterranean Sea : an oceanographic perspective. CIEMS Workshop Monograph 31–41. doi:10.13140/RG.2.1.2315.3760

Zambianchi, E., Trani, M., Falco, P., 2017. Lagrangian Transport of Marine Litter in the Mediterranean Sea. Frontiers in Environmental Science 5, 1–15. doi:10.3389/fenvs.2017.00005

Wright, S.L., Thompson, R.C., Galloway, T.S., 2013. The physical impacts of microplastics on marine organisms: a review. Environ. Pollut. 178, 483-492. https://doi.org/10.1016/j.envpol.2013.02.031

Figures

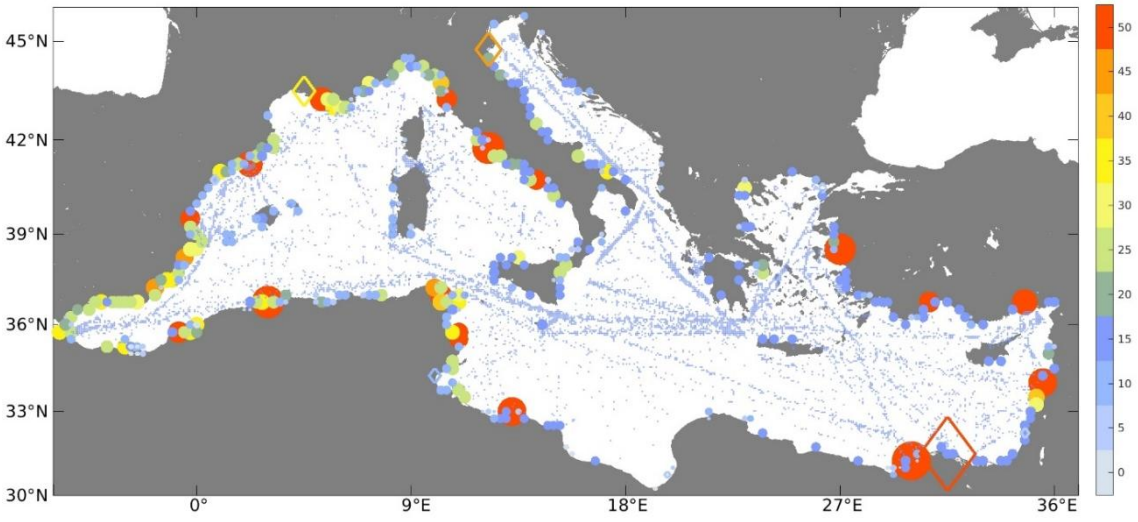
45°N
42°N
39°N
36°N
33°N
30°N
0°
9°E
18°E
27°E
36°E
50
45
40
35
30
25
20
15
10
5
0

Figure 1. Spatial distribution of initial marine litter concentrations (in kg/km^2) for the three simulations. Circle filled points indicate cities, diamonds indicate rivers and points over the sea indicate the ship lines.

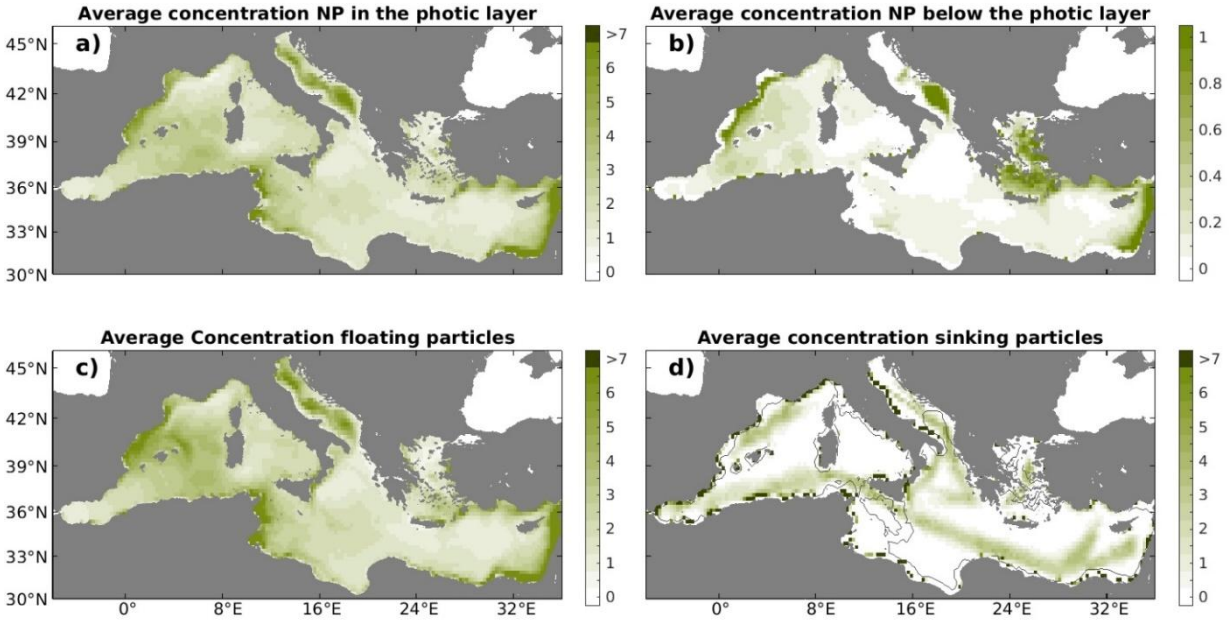

Figure 2. Average marine litter concentration for the three simulations: **a)** Neutral particles above the base of the photic layer. **b)** Neutral particles below the base of the photic layer. **c)** Floating particles. **d)** Sinking particles, the black thin line indicates the 400 m isobath. Units are kg/km^2. Note that the range of values in (b) is different.

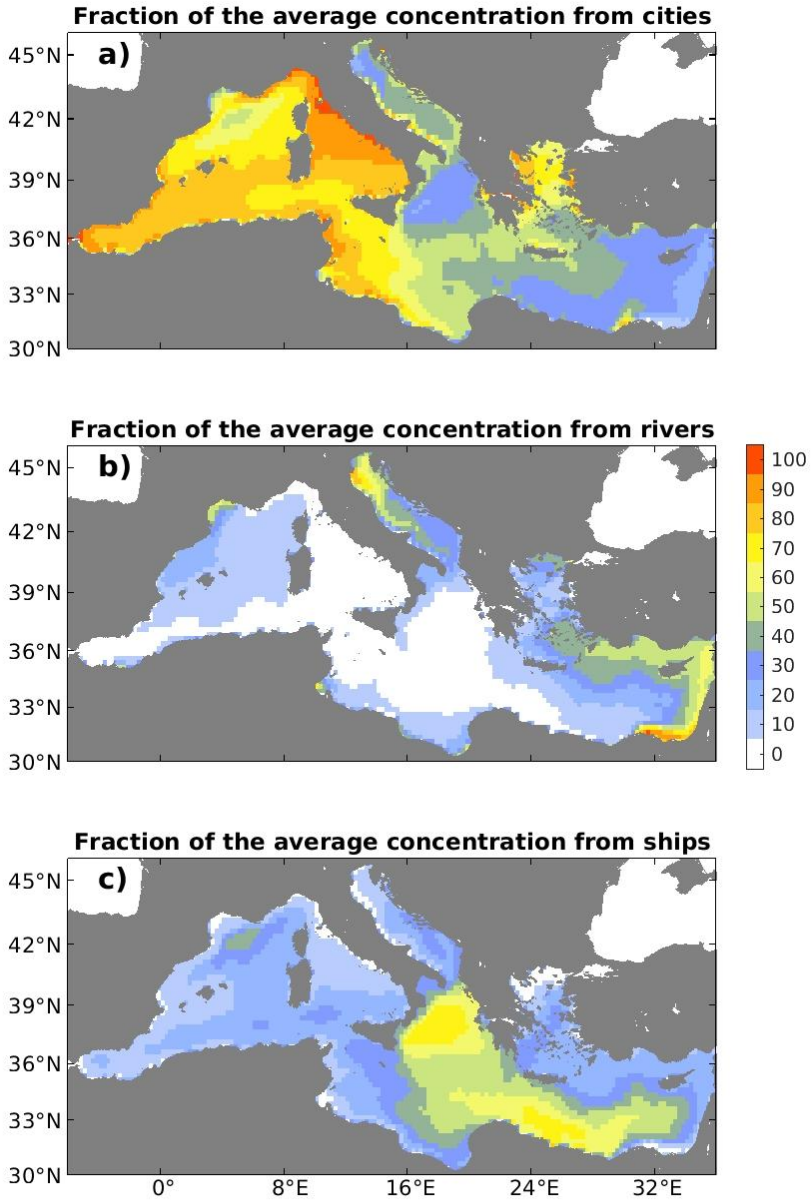

Figure 3. Contribution of the three marine litter sources. a) cities, b) rivers and c) ships, to the averaged marine litter concentration showed in Figure 2a.

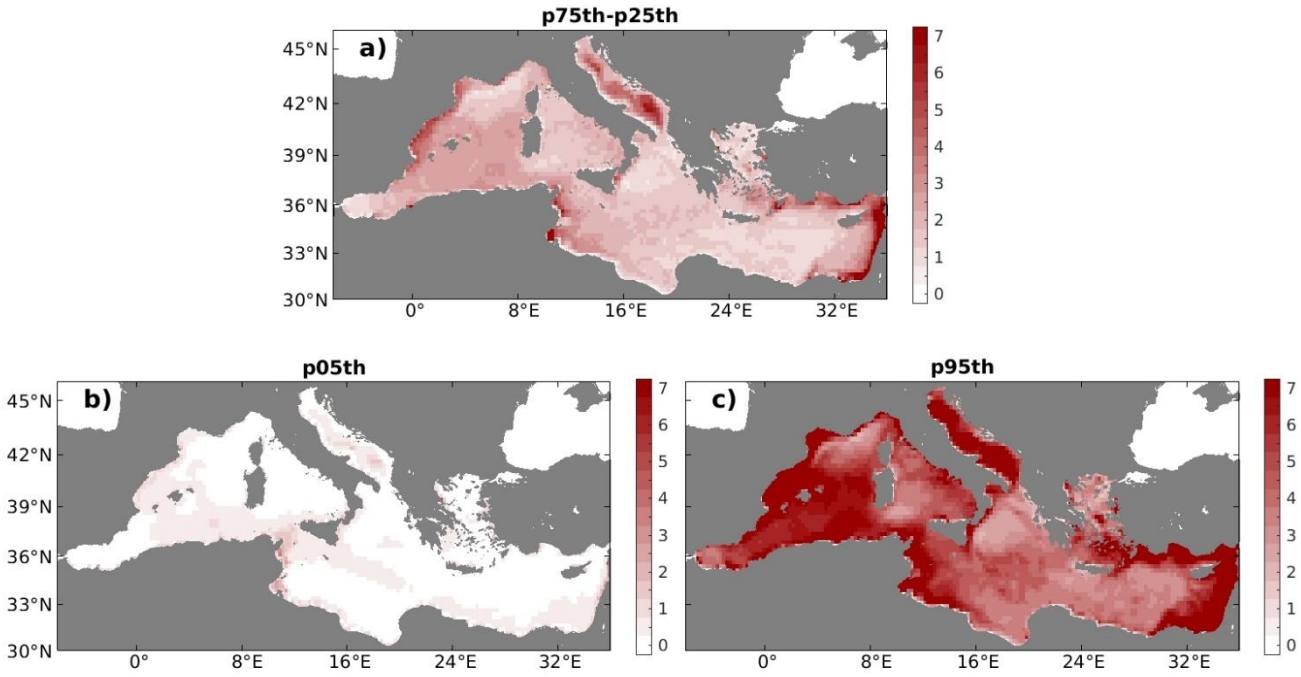

Figure 4. Quantiles of the marine litter concentration. a) Interquartile range (p75th – p25th), b) p05th and c) p95th.

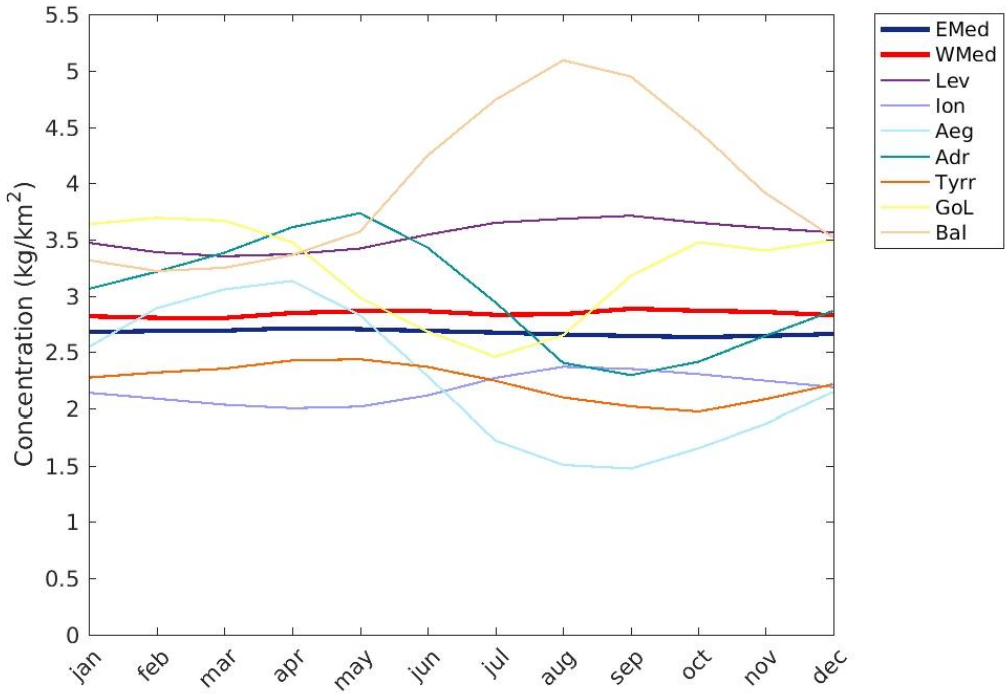

Figure 5. Seasonal cycles of the ML concentration in the different sub-basins: Eastern Mediterranean (EMed, dark blue), Western Mediterranean (WMed, red), Levantine Basin (Lev, purple), Ionian Sea (ion, light blue), Aegean Sea (Aeg, cyan), Adriatic Sea (Adr, green), Tyrrhenian Sea (Tyrr, orange), Gulf of Lions (GoL, yellow) and Balearic Sea (Bal, salmon).

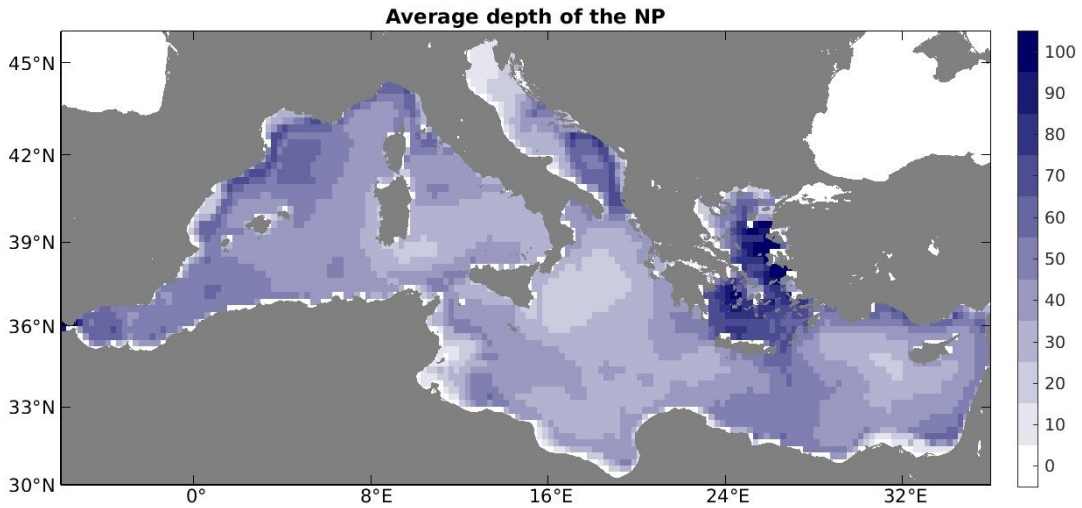

Figure 6. Average of the vertical distribution of neutral particles (in meters (m)).

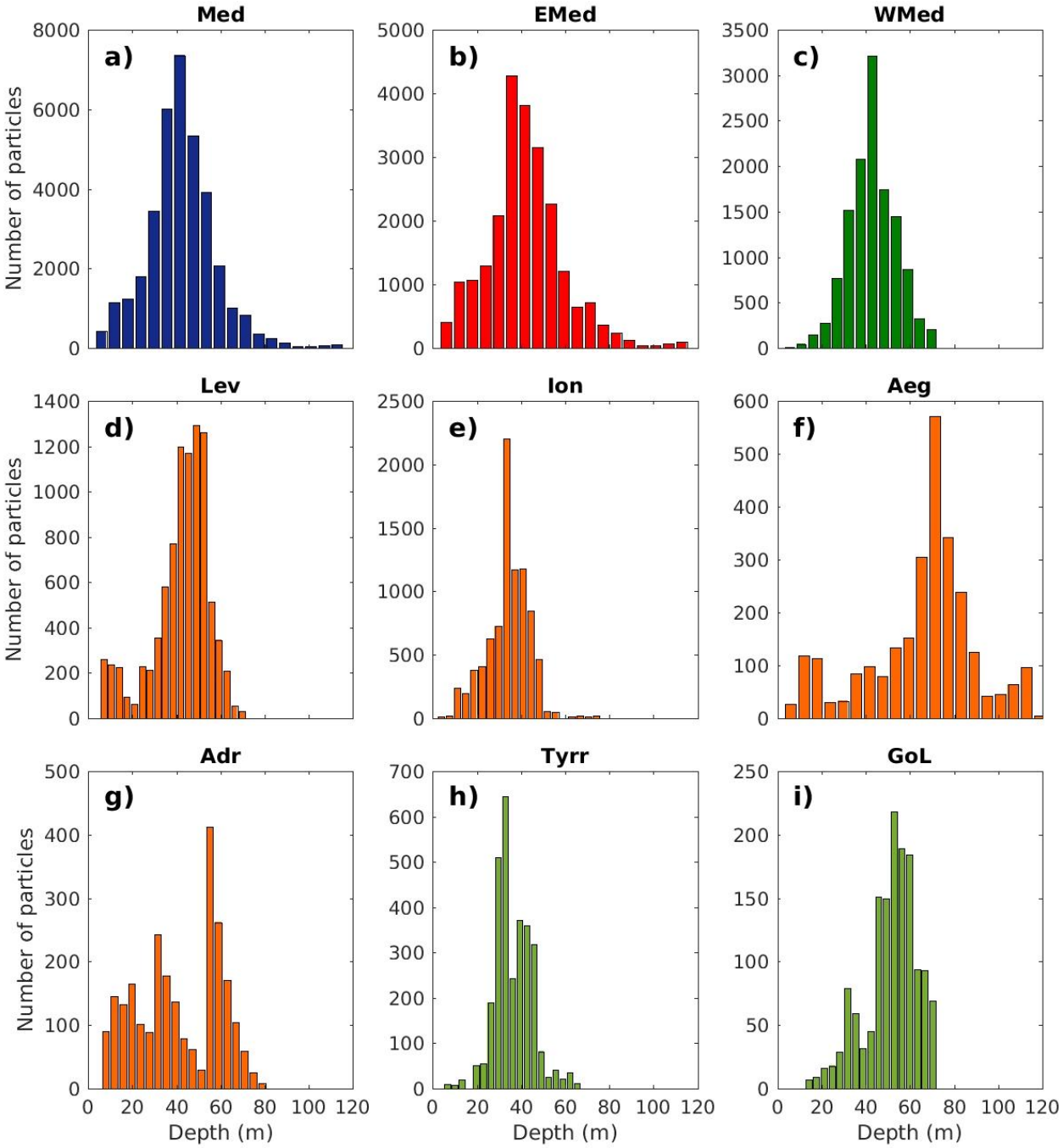

Figure 7. Histograms of the average depth distribution of particles in the different sub-basins. a) Mediterranean Sea, b) Eastern Mediterranean, c) Western Mediterranean, d) Levantine Basin, e) Ionian Sea, f) Aegean Sea, g) Adriatic Sea, h) Tyrrhenian Sea and i) Gulf of Lions. For clarity, only the first 120 m are shown as far as the contribution below is very small.

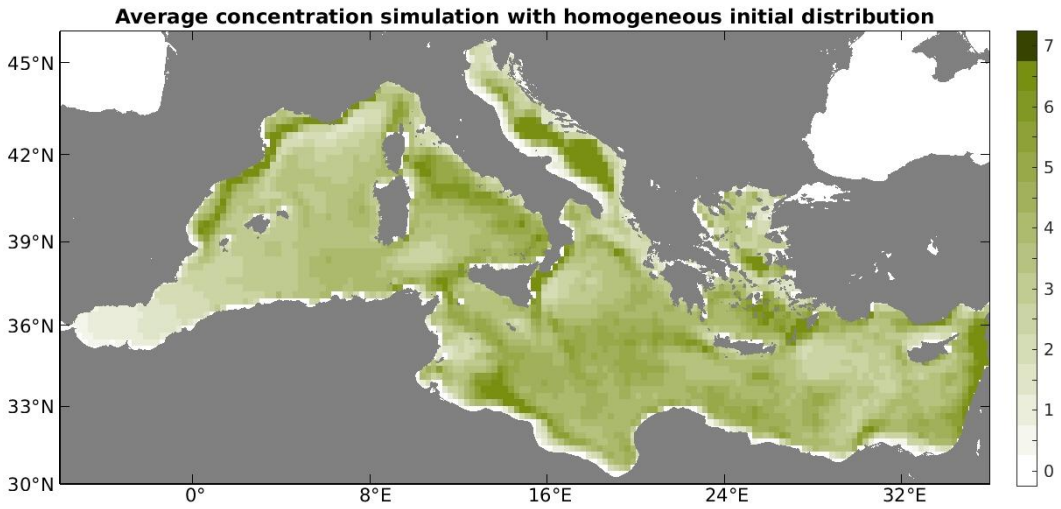

Figure 8. Average concentration for the simulation starting from a homogeneous particle distribution over the whole basin. Units are kg/km^2.

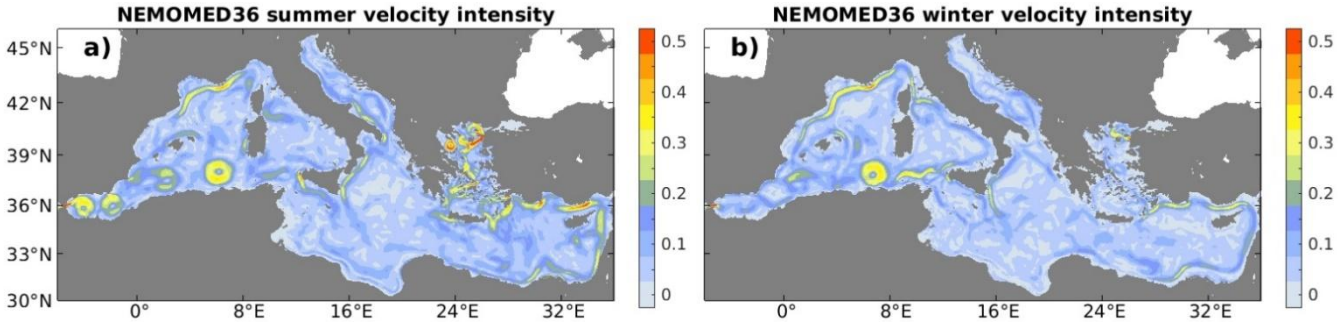

Figure 9. Model average current intensity for a) summer and b) winter months. Units are m/s^{-1}

Wright, S.L., Thompson, R.C., Galloway, T.S., 2013. The physical impacts of microplastics on marine organisms: a review. Environ. Pollut. 178, 483-492. https://doi.org/10.1016/j.envpol.2013.02.031

Tables

Simulation	Short name	Integration time	Vertical velocity
Neutral particles	S-NP	120 sim of 1yr	Given by RCM
Floating particles	S-FP	120 sim of 1yr	0
Sinking particles	S-SP	120 sim of 1yr	-10^{-2} m·s^{-1} added to RCM vertical velocity field

Table 1. Summary of the main characteristics of the three simulations analyzed.

Figure 1

Click here to download high resolution image

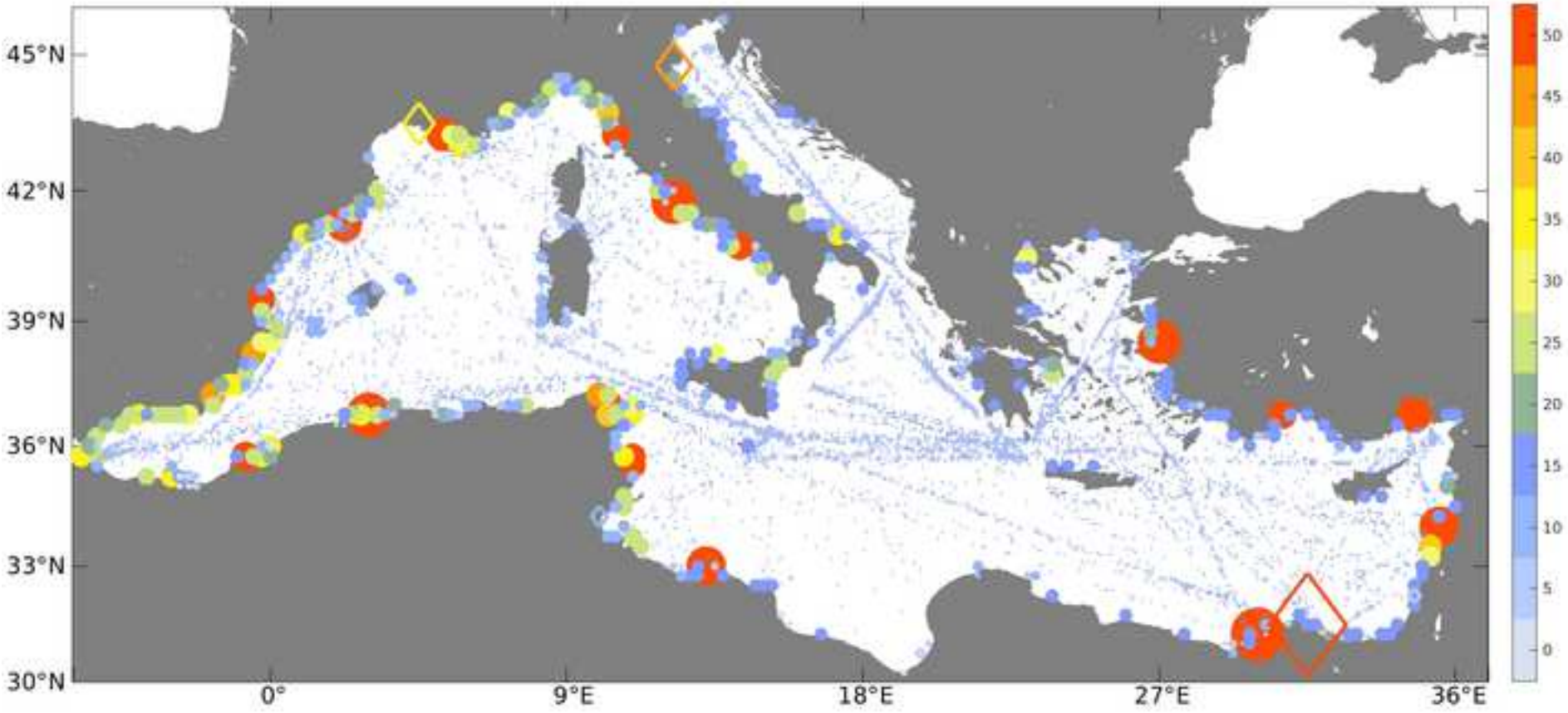

Figure 2

Click here to download high resolution image

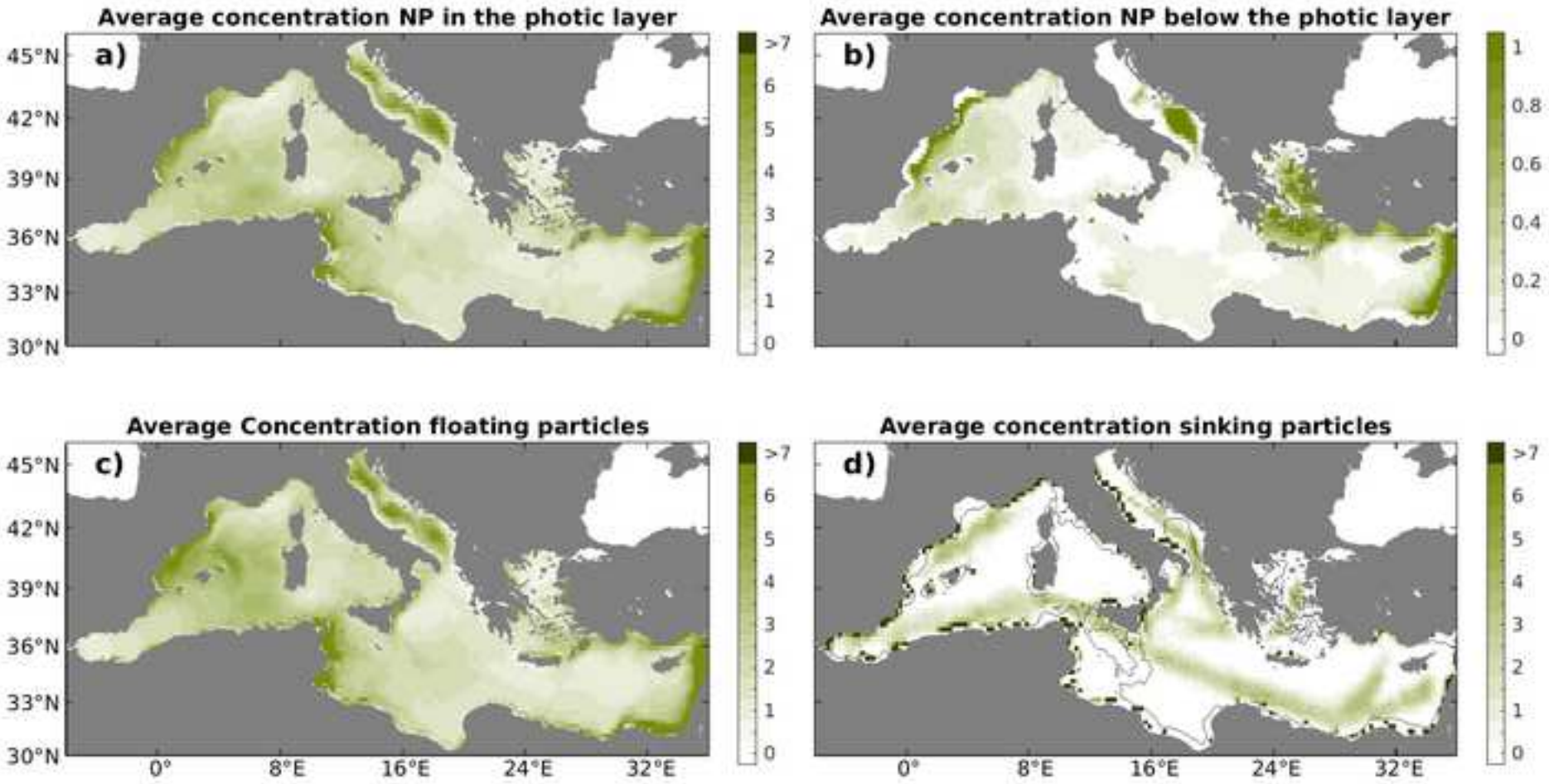

Figure 3

Click here to download high resolution image

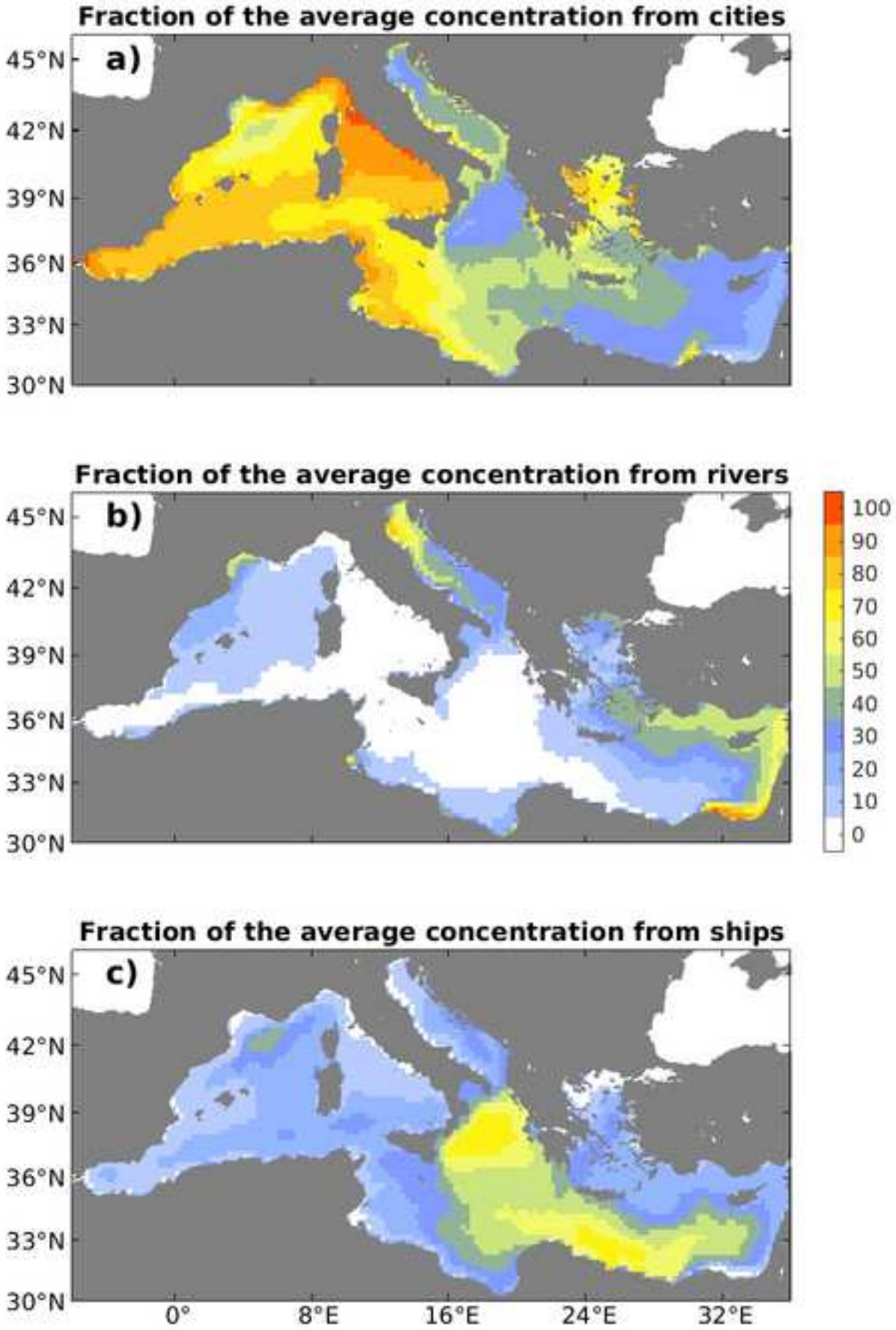

Figure 4

Click here to download high resolution image

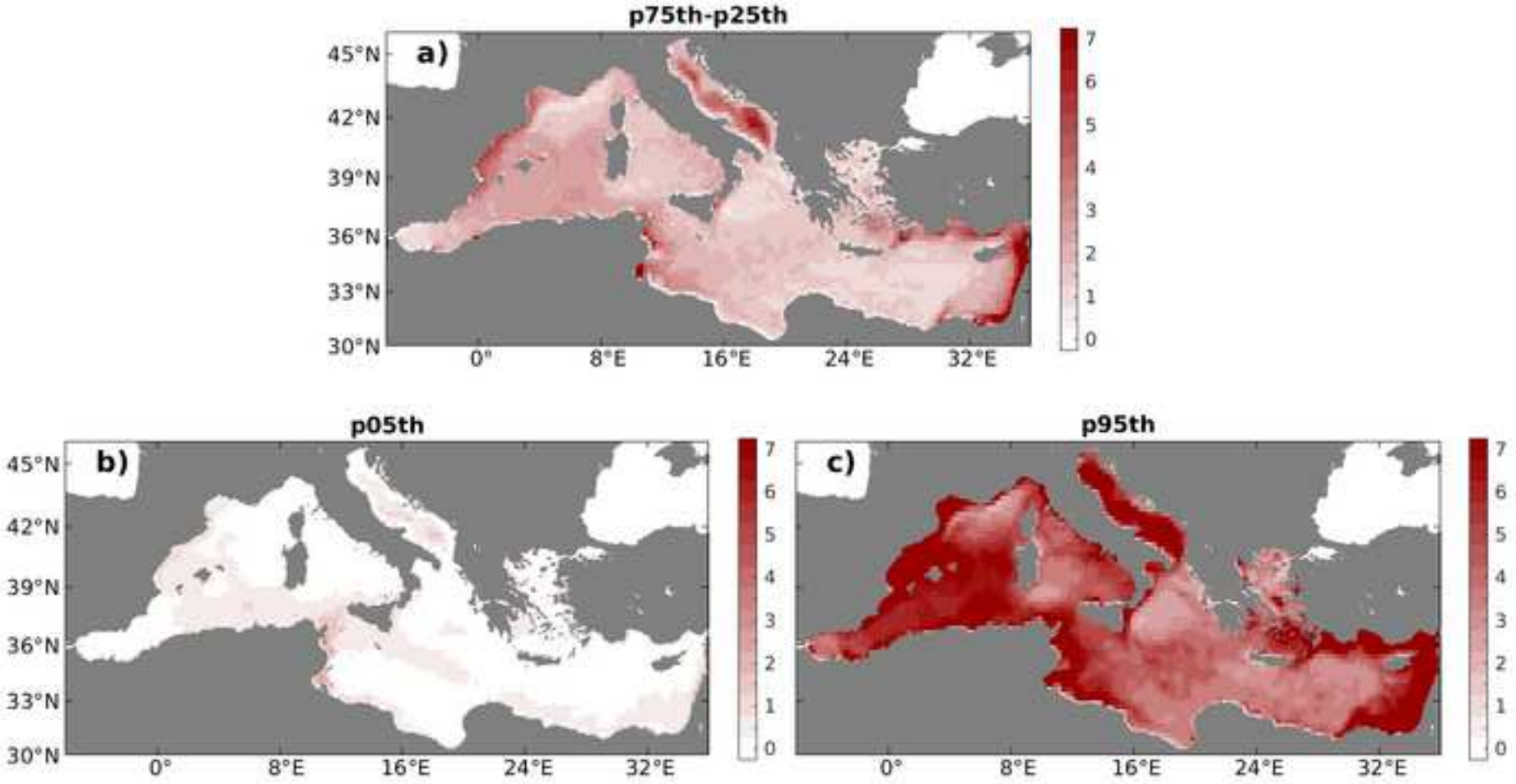

Figure 5

Click here to download high resolution image

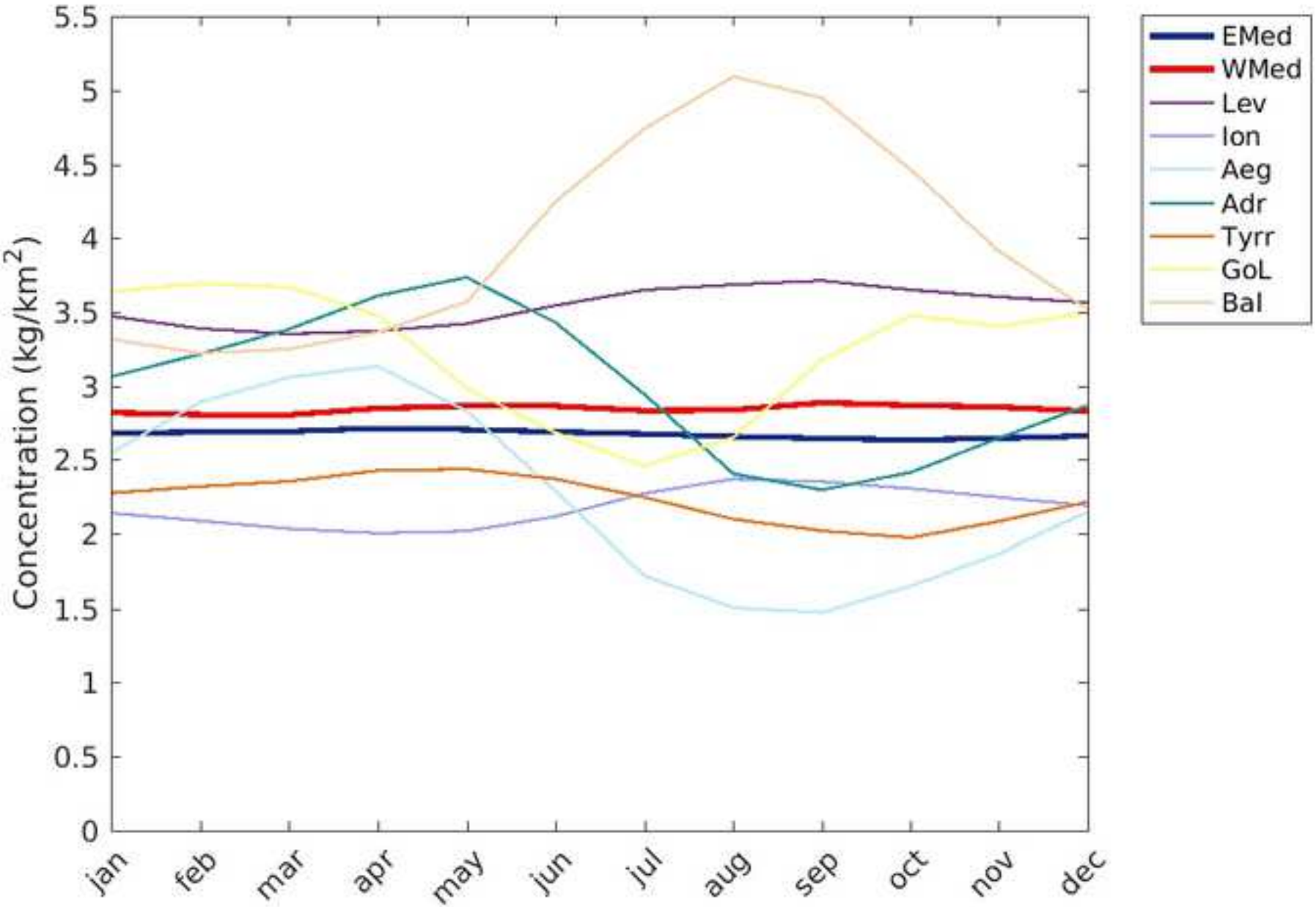

Figure 6

Click here to download high resolution image

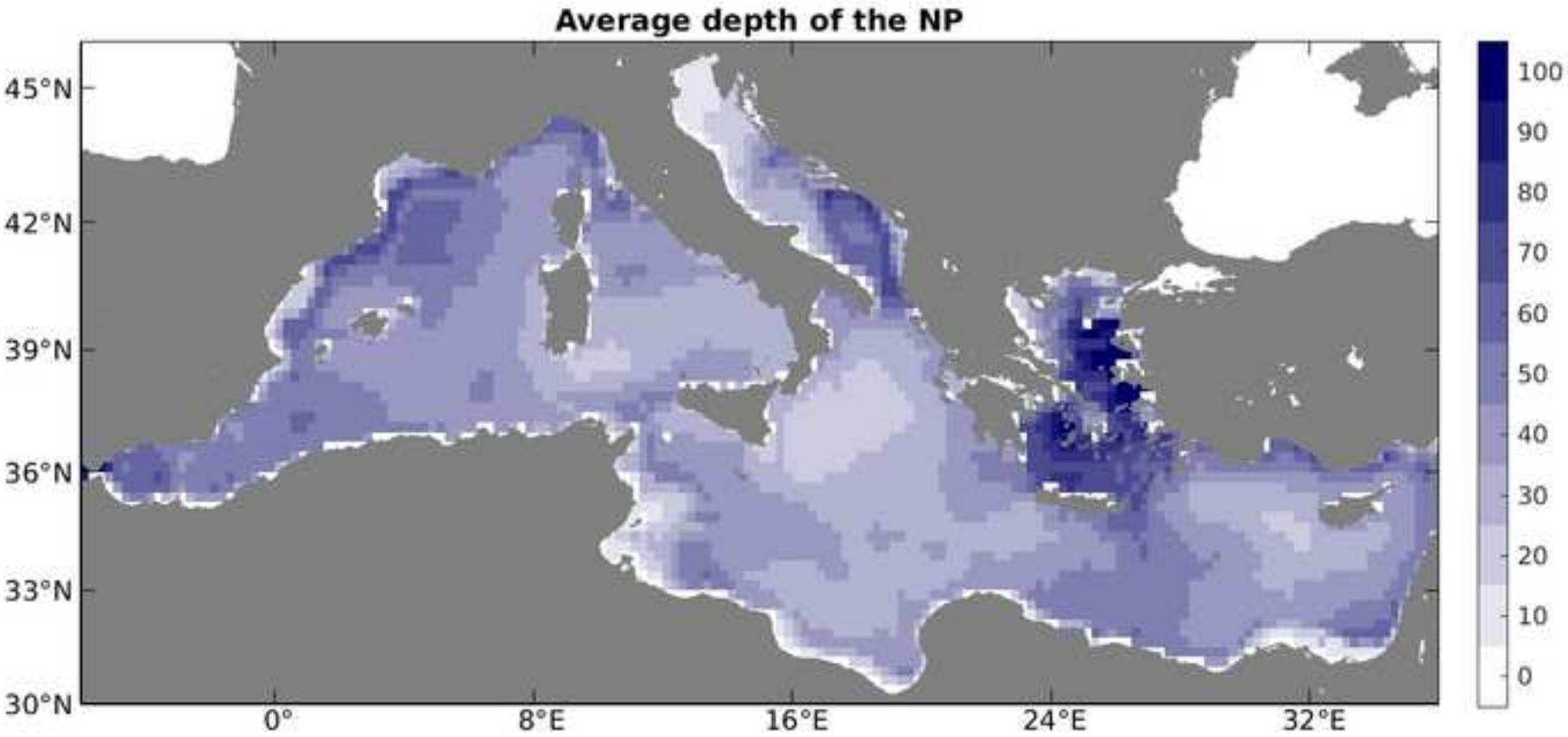

Figure 7

Click here to download high resolution image

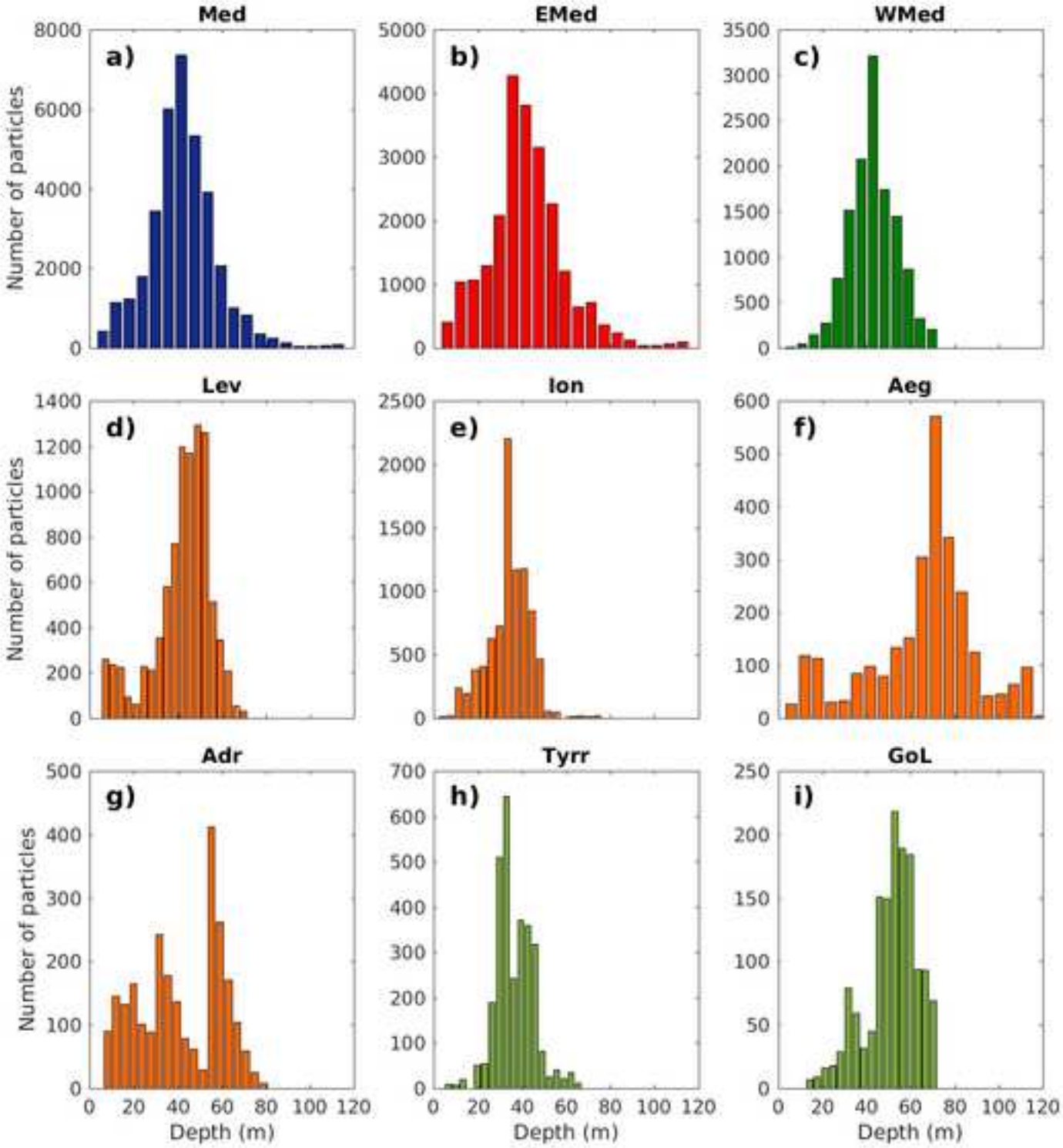

Figure 8

Click here to download high resolution image

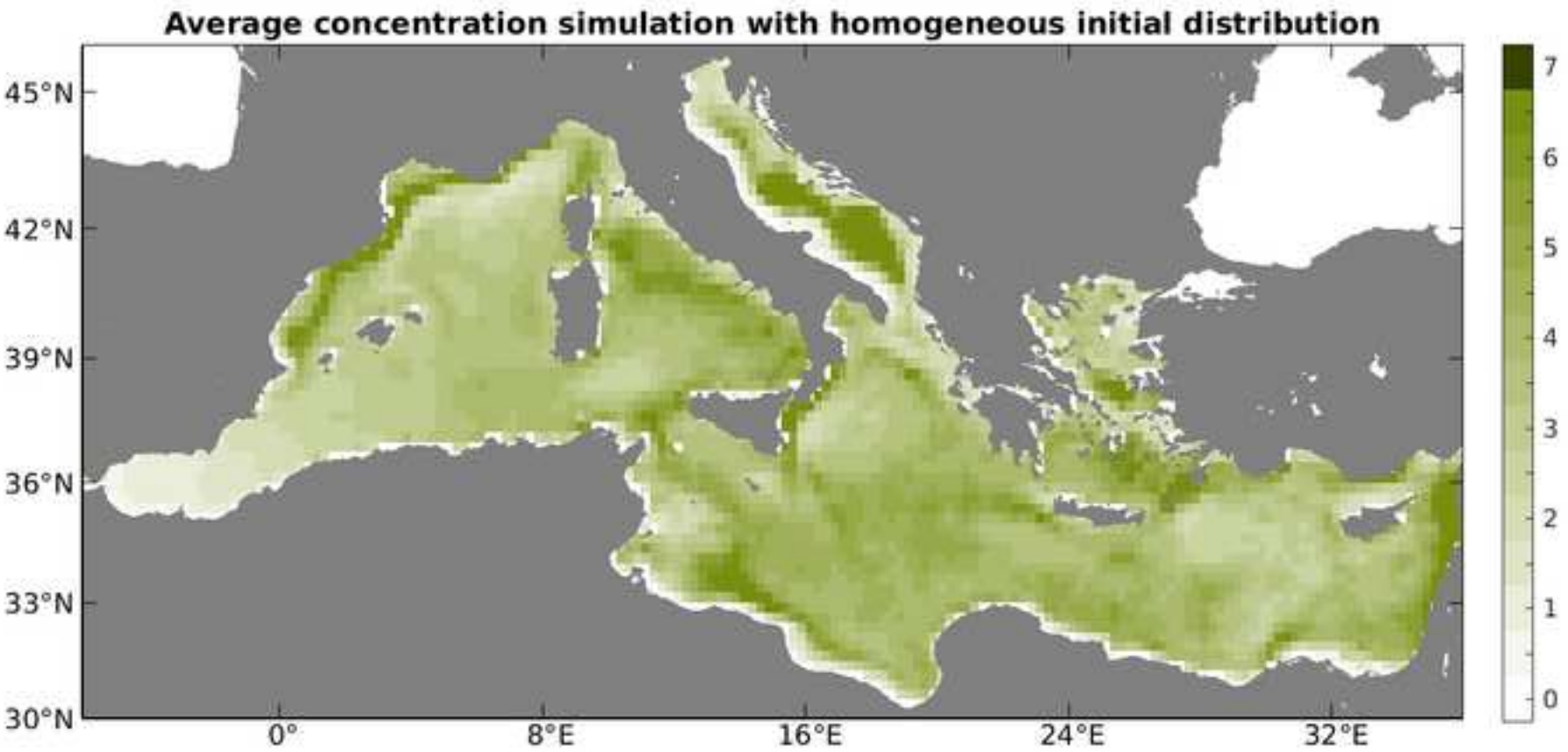

Figure 9

Click here to download high resolution image

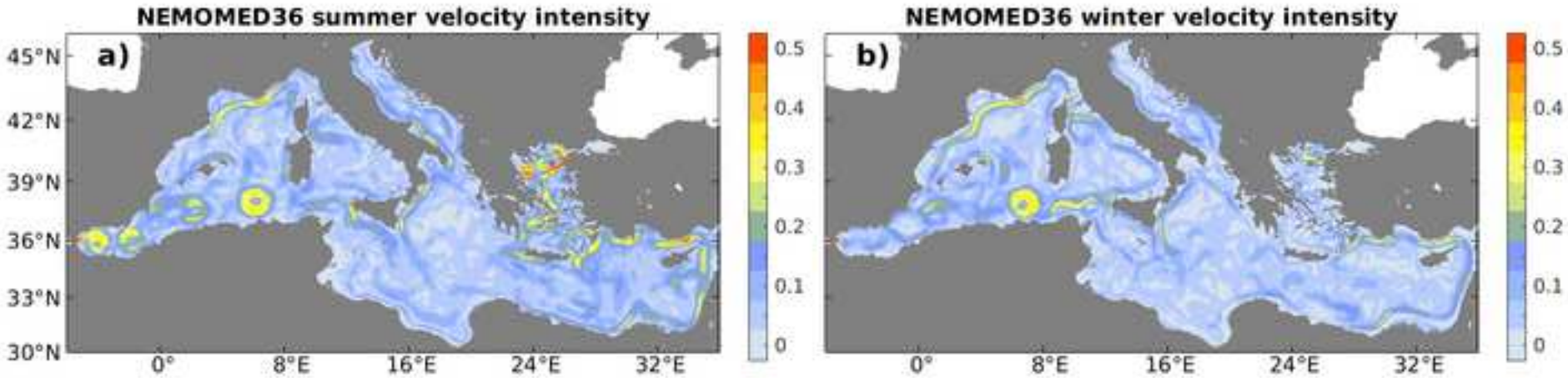

***Declaration of Interest Statement**

Declaration of interests

☒ The authors declare that they have no known competing financial interests or personal relationships that could have appeared to influence the work reported in this paper.

☐The authors declare the following financial interests/personal relationships which may be considered as potential competing interests:

***Credit Author Statement**

3D hotspots of marine litter in the Mediterranean: a modeling study

Javier Soto-Navarro[1], Gabriel Jordá[2], Salud Deudero[2], Carme Alomar[2], Ángel Amores[1] and Montserrat Compa[2].

Javier Soto-Navarro: Writing - Original Draft, Methodology, Data Curation, Formal Analysis, Conceptualization

Gabriel Jordá: Conceptualization, Writing - Review & Editing, Methodology, Formal Analysis Supervision.

Salud Deudero: Conceptualization, Writing - Review & Editing, Funding acquisition

Carme Alomar: Conceptualization, Writing - Review & Editing.

Ángel Amores: Software.

Montserrat Compa: Conceptualization, Writing - Review & Editing.